Science of the Total Environment 867 (2023) 161475

Contents lists available at ScienceDirect

Science of the Total Environment

journal homepage: www.elsevier.com/locate/scitotenv

The HL-60 human promyelocytic cell line constitutes an effective in vitro model for evaluating toxicity, oxidative stress and necrosis/apoptosis after exposure to black carbon particles and 2.45 GHz radio frequency

Rosa Ana Sueiro Benavides [a], José Manuel Leiro-Vidal [a], J. Antonio Rodriguez-Gonzalez [b], Francisco J. Ares-Pena [b], Elena López-Martín [c,*]

[a] Institute of Research in Biological and Chemical Analysis, IAQBUS, University of Santiago de Compostela, Santiago de Compostela, Spain
[b] Department of Applied Physics, Santiago de Compostela School of Physics, University of Santiago de Compostela, Santiago de Compostela, Spain
[c] Department of Morphological Sciences, Santiago de Compostela School of Medicine, University of Santiago de Compostela, Santiago de Compostela, Spain

HIGHLIGHTS

- RF+ BC increase ROS production and have an oxidant-antioxidant effect on HL-60 cells.
- RF or BC exposure activates expression of the anti-apoptotic gene BCL2a in HL-60 cells.
- Cell necrosis due to BC was manifested at 24 h, while cell death (necrosis and/or apoptosis) due to irradiation and/or BC lasted up to 48 h.
- Interaction between RF and BC enhanced cell toxicity in the promyelocytic cell line.

GRAPHICAL ABSTRACT

The interaction between BC and RF triggers oxidative stress and modifies the immune response in the human promyelocytic cell line, thereby activating necrosis/apoptosis and causing prolonged cell toxicity.

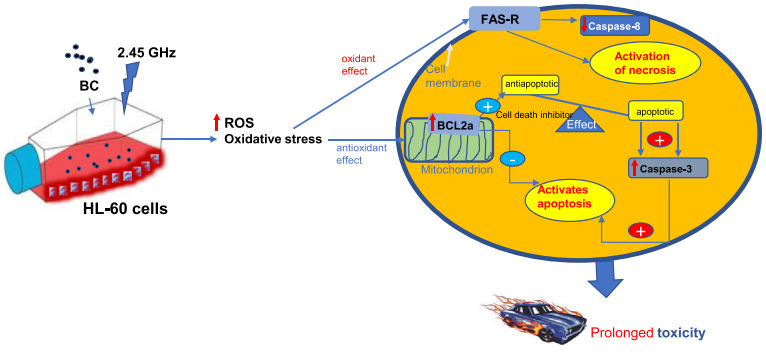

ARTICLE INFO

Editor: Jianmin Chen

Keywords:
HL-60 promyelocytic cell line
Black carbon
Electromagnetic fields
Gigahertz transverse electromagnetic cell
Specific absorption rate
Necrosis/apoptosis
BCL2a/FASR/CASP3 genes
Caspase-3/8 proteins

ABSTRACT

The cellular and molecular mechanisms by which atmospheric pollution from particulate matter and/or electromagnetic fields (EMFs) may prove harmful to human health have not been extensively researched. We analyzed whether the combined action of EMFs and black carbon (BC) particles induced cell damage and a pro-apoptotic response in the HL-60 promyelocytic cell line when exposed to 2.45 GHz radio frequency (RF) radiation in a gigahertz transverse electromagnetic (GTEM) chamber at sub-thermal specific absorption rate (SAR) levels. RF and BC induced moderately significant levels of cell damage in the first 8 or 24 h for all exposure times/doses and much greater damage after 48 h irradiation and the higher dose of BC. We observed a clear antiproliferative effect that increased with RF exposure time and BC dose. Oxidative stress or ROS production increased with time (24 or 48 h of radiation), BC dose and the combination of both. Significant differences between the proportion of damaged and healthy cells were observed in all groups. Both radiation and BC participated separately and jointly in triggering necrosis and apoptosis in a programmed way. Oxidative-antioxidant action activated mitochondrial anti-apoptotic BCL2a gene expression after 24 h irradiation and exposure to BC. After irradiation of the cells for 48 h, expression of FASR cell death receptors was activated, precipitating the onset of pro-apoptotic phenomena and expression and intracellular activity of caspase-3 in the mitochondrial pathways, all of which can lead to cell death. Our results indicate that the interaction between BC and RF modifies the immune response in the human promyelocytic cell line and that these cells had two

* Corresponding author.
E-mail addresses: rosaana.sueiro@usc.es (R.A.S. Benavides), josemanuel.leiro@usc.es (J.M. Leiro-Vidal), ja.rodriguez@usc.es (J.A. Rodriguez-Gonzalez), francisco.ares@usc.es (F.J. Ares-Pena), melena.lopez.martin@usc.es (E. López-Martín).

http://dx.doi.org/10.1016/j.scitotenv.2023.161475
Received 12 May 2022; Received in revised form 21 December 2022; Accepted 4 January 2023
Available online 9 January 2023

fates mediated by different pathways: necrosis and mitochondria-caspase dependent apoptosis. The findings may be important in regard to antimicrobial, inflammatory and autoimmune responses in humans.

1. Introduction

Air pollution from both indoor and outdoor sources is estimated to have contributed to at least five million premature deaths (GBD, 2016). There is evidence that the black carbon (BC) particles found in atmospheric pollution can have harmful effects on human health and that some environmental particles emitted by anthropogenic activities may be toxic (Offer et al., 2022). Existing data also relate BC exposure to cancer, respiratory diseases and cardiovascular disorders (Rituraj and Thakur, 2017). BC particles are the unwanted by-products of the incomplete combustion of carbon-containing materials (Long et al., 2013; Watson and Valberg, 2001) and range from about 10 nm to 1 mm in size (Wang et al., 2014; China et al., 2013). Recent long-term follow-up research has shown an increased health risk (Yang et al., 2021) and evidence of increased of toxicity (Magalhaes et al., 2018) from BC exposure. Accordingly, the high oxidative potential (Shang et al., 2021) of carbonaceous particles should be given greater attention in experimental measurements involving air (Salas-Sánchez et al., 2020, as well as in the development of pollution mitigation scenarios and policy measures (Chowdhury et al., 2022). Inhaled pollutants have been shown to induce redox-sensitive signaling by generating free-radical oxidants (reactive oxygen species) in cellular and acellular experimental systems. Similarly, ambient particulate matter has been found to cause oxidative stress and reduce endogenous antioxidants (Ghio et al., 2012).

In another area of interest, the widespread use of electromagnetic fields (EMFs) emitted at 2.45 GHz frequency in industrial and medicinal technology and in daily life has generated concern in society and among health authorities regarding possible health hazards from continued exposure to the radiation (Bosch-Capblanch et al., 2022; Roosli et al., 2010). Production of reactive oxygen species (ROS) that may cause cellular or systemic oxidative stress in cells and animals has frequently been found to be influenced by exposure to EMF radiation (Schuermann and Mevissen, 2021), though it is dependent on the cell type and exposure time (Zielinski et al., 2020). This has been described for Wi-Fi frequencies of 2.45 GHz in tissues and organs (Pall, 2018), in vivo animal models (Akkaya et al., 2019; Kamali et al., 2018; Tök et al., 2014) and in vitro cell models (Özsobacı et al., 2018; Çiğ and Nazıroğlu, 2015; Nazıroğlu et al., 2012). Effects of oxidative stress have also been observed at 900 MHz (Sun et al., 2017), 1800 MHz (Hou et al., 2015) and other frequencies (Kim et al., 2021). The World Health Organization (WHO) recently commissioned a diverse group of radio frequency (RF) experts to prioritize the potential health outcomes or biological effects of exposure to RF electromagnetic fields and to provide a rationale for their choices. This commission determined that changes in oxidative stress biomarkers was one of the exposure outcomes that should be prioritized (Verbeek et al., 2021). Acceleration of these mechanisms due to non-ionizing radiation could significantly affect the aetiopathogenesis and evolution of cancer (Panagopoulos et al., 2021) and neurodegenerative diseases (Zielinski et al., 2020).

In this study, we studied the mechanisms underlying the cellular response and/or potentially toxicological effects on immature granulocytes (precursor cells) in the HL-60 promyelocytic cell line exposed to a combination of two environmental pollutants: black carbon particles and electromagnetic radiation. The HL-60 promyelocytic cell line was used as an in vitro model to facilitate preliminary evaluation of the health risks and impact on the immediate immune response (Glencross et al., 2020) from toxic agents (Verdon et al., 2021) that alter air quality. Phagocytic cells form a key component in the acute inflammatory response triggered by contact with environmental particles (Johnston et al., 2015; Goncalves et al., 2011). Use of in vivo experimental models (usually rodents) has shown that neutrophils infiltrate target sites where the particles accumulate, including the lungs (Baisch et al., 2014; Jacobsen et al., 2009) pleural cavity (Arnoldussen et al., 2018; Murphy et al., 2013) and peritoneal cavity (Poland et al., n.d.) following administration via different routes (inhalation, intratracheal instillation, intrapleural and intraperitoneal injection). The HL-60 cell line can be used as an in vitro model to provide relevant information in a short time about the cell response to potential toxins in relation to the composition and concentration of environmental particles (Johnston et al., 2015). Certain components of environmental particles have been reported to alter the levels of oxidative stress and cause apoptosis by inducing synergistic toxic effects in rat alveolar macrophages (Guan et al., 2020) and in organs (e.g. kidney) via both mitochondria-dependent and independent pathways (Sarkar et al., 2011). Thus, HL-60 cell lines may also provide a tiered testing strategy for hazard assessment of environmental particles without the need to use rodents or other animals (Verdon et al., 2021). Cell-based studies that are less expensive and provide results more quickly support efforts to reduce, replace and refine the use of laboratory animals. Similarly, optimization and promotion of in vitro techniques should align with the 3Rs principles (replacement, reduction, refinement) guiding animal research (Russell and Burch, 2005). In previous studies, promyelocytic HL-60 cells displayed great vulnerability to the normothermic effect of microwave radiation (Asano et al., 2017a), which caused cell death due to mitochondrial dysfunction via caspase-independent apoptosis (Asano et al., 2017b). However, it has also been shown that the effect of exposure to 2.45 GHz RF EMF for 4 and 24 h did not affect neutrophil chemotaxis or phagocytosis in differentiated human HL-60 cells (Koyama et al., 2015).

Innate immune cells in the respiratory tract, such as macrophages and neutrophils, are the first to respond to inhaled pathogens (Glencross et al., 2020). The interaction between non-ionizing radiation and BC particles causes a dramatic increase in previously reported cytotoxicity in the RAW macrophage cell line and is accompanied by pro-apoptotic activation of caspase-3, prolonged phagocytosis and amplification of the macrophage inflammatory response (Sueiro-Benavides et al., 2021). Human HL-60 promyelocytic cells have been used to study inflammatory cells (Wang et al., 2020; Kobayashi et al., 2017). The HL-60 cell line can be differentiated into granulocyte-like cells, monocyte/macrophage-like cells and eosinophils (after treatment with certain chemicals) (Birnie, 1988).

In this experimental study, we directly assessed the response of HL-60 promyelocytic cells to two environmental stress agents, with no prior induction by chemical agents that could modify the response in any way. Understanding the immune response to environmental toxins and the consequences for human health is key to any relevant risk assessment (Johnston et al., 2015). Our study hypothesis was that radiation can modulate levels of oxidative stress and alter the activity of promyelocytic cells exposed to BC, thereby inducing cytotoxicity. To test our hypothesis, the HL-60 promyelocytic cell line was exposed to 2.45 GHz RF for 8, 24 or 48 h in a gigahertz transverse electromagnetic (GTEM) cell test chamber. Several innate immune functions were subsequently studied and evaluated, including the viability, antiproliferative effect, production of reactive oxygen species (ROS) and necrosis and/or apoptosis. ROS production was measured using the nitroblue tetrazolium (NBT) assay. Necrosis was measured by caspase-3 gene expression and apoptosis was measured by the activity of intracellular caspases 3 and 8. This enabled us to determine whether one or both toxic agents triggered the pro-apoptotic mechanisms and pathways that induce cell death. In addition, we examined activation of BCL2a gene expression in relation to the mitochondria-dependent intrinsic pathway and activation of FASR gene expression in relation to the extrinsic pathway.

2. Materials and methods

2.1. Cell culture

Human promyelocytic leukemia (HL-60) cells, which are routinely cultured in Iscove's Modified Dulbecco's Medium (IMDM; GibcoTM, Paisley,

UK), were supplemented with 3.024 mg/L NaHCO3 and 10 % heat-inactivated foetal bovine serum (FBS; GibcoTM). The cells were maintained at sub-confluent density at 37 °C in a humidified atmosphere containing 5 % CO_2. Two different culture media were used: 1) In the sub-confluent cultures (70–90 % cover) of the HL-60 cells, 90 % of the old IMDM medium was removed. The cells were transferred to a new 75 cm^2 flask (Thermo Fisher Scientific, Waltham, MA, USA) at reduced concentrations of between 1/3 and 1/6, depending on the initial cell concentration, and fresh medium was added. The flasks were incubated horizontally as before (5 % CO_2 and 37 °C). The fresh medium was warmed to 37 °C before use. 2) Leibovitz L-15 medium (GibcoTM) was used during irradiation as it does not contain bicarbonate as a buffer. Foetal bovine serum (FBS) was also added to the L-15 medium as a growth factor.

2.2. Characteristics of the particulate samples

The BC used in the study was glassy spherical BC powder, measuring 0.4–12 μm (Thermo Fisher Scientific MFCD00133992 Kandel, Germany). The BC was prepared as 1 g/mL stock solutions in dimethyl sulphoxide (DMSO) and was held in darkness at room temperature until use. The stocks were diluted in IMDM or L-15 medium containing 10 % FBS immediately prior to use, to obtain the final concentrations required for each assay.

2.3. Experimental design

The experimental groups (G) were established according to the following experimental design:

- G1: Non-irradiated control cell cultures examined after 8 and 24 h (HL-60 no RAD 8 or 24 h).
- G2: Cell cultures exposed to BC at concentrations of 50 μg/mL (G2A) and 150 μg/mL (G2B), without irradiation, examined after 8 and 24 h (HL-60 50 BC μg/mL + no RAD 24 h or HL-60 150 BC μg/mL + no RAD 8 or 24 h).
- G3: Cell cultures irradiated for 8 or 24 h (HL-60 RAD 8 or 24 h).
- G4: Cell cultures exposed to BC at concentrations of 50 μg/mL (G4A) and 150 μg/mL (G4B) BC and irradiated for 8 or 24 h (HL-60 50 BC μg/mL RAD 8 or 24 h).
- G5: Non-irradiated control cultures examined after 48 h (G5) (HL-60 no RAD 48 h)
- G6: Cell cultures exposed to BC at concentrations of 50 μg/mL (G6A) or 150 μg/mL (G6B), without irradiation, examined after 48 h (HL-60 50 BC μg/mL + no RAD 48 h or HL-60 150 BC μg/mL + no RAD 48 h).
- G7: Cell cultures irradiated for 48 h (HL-60 RAD 48 h).
- G8: Cell cultures exposed to BC at concentrations of 50 μg/mL (G8A) or 150 μg/mL (G8B) and irradiated for 48 h (HL-60 50 BC μg/mL + RAD or HL-60 150 BC μg/mL + RAD).

2.4. Experimental irradiation system

Cells were placed in 25 cm^2 culture flasks (Thermo Fisher Scientific, Waltham, MA) and the culture medium was replaced with L-15 supplemented with 10 % inactivated FBS (PAN Biotech, Dorset, UK). Independent HL-60 cell cultures were then individually exposed to radiation in the GTEM chamber (three cell cultures per group) at the point of maximum field uniformity, with the culture flask placed horizontally and the flask cup oriented towards the source of radiation.

2.5. Analysis of cell viability

HL-60 cell viability was determined by trypan blue exclusion, after staining the cells with trypan blue vital dye (Sigma-Aldrich St. Louis, MO, USA). After the 24 and 48 h treatments, aliquots of 1×10^5 cells from each experimental group were collected in a screw-cap test tube and centrifuged at 450 ×*g* for 5 min. The cell pellet was re-suspended in 500 μl of L15 medium without serum, and 100 μl of 0.4 % trypan blue stain in sterile phosphate buffered saline (PBS; pH 7.2) was then added to each cell suspension. The mixture was incubated for 5 min at room temperature. Viable cells were counted in a Neubauer haemocytometer under a light microscope (Nikon Eclipse E-600, Japan). Trypan blue is reactive because the chromophore is negatively charged and does not interact with the cell unless the membrane is damaged. Therefore, all cells that exclude the dye are viable. The cell suspension was inoculated in the haemocytometer, and the cells in 4 upper quadrants and 4 lower quadrants each measuring 1x1mm were then counted. Total live cells (that did not take up the trypan blue stain) and dead cells (not stained) were counted, and the percentage of live cells in each group was calculated relative to the total number of cells in the 4 upper and 4 lower quadrants. The viability of each group was thus measured, with 6 samples per group.

Trypan blue staining was also used to study the anti-proliferative effect of radiation from a 2.45 GHz electromagnetic field on the HL-60 promyelocytic cell line. These effects were calculated according to the following formula:

Percentage inhibition of cell growth = [(Control group $_{\text{Number of cells}}$ − EMF $_{\text{Number of cell}}$ or $BC_{50\text{ or }150\mu g}$ + EMF $_{\text{Number of cell}}$ or $BC_{50\text{ or }150\mu g}$ without EMF $_{\text{Number of cells}}$) / Control group $_{\text{Number of cells}}$] × 100 (Barati et al., 2021).

2.6. NBT reduction to determine cell differentiation and ROS production

For this procedure, 2×10^6 treated and untreated HL-60 cells / mL were washed twice in HBSS buffer. The pellet was resuspended in 1 mL of HBSS buffer, and 1 mL of a fresh solution of 0.2 % nitroblue tetrazolium (NBT) in HBSS was added. The cells were incubated for 60 min at 37 °C and then centrifuged at 1500 rpm for 5 min. The cell pellet was resuspended in 100 μL of HBSS and stained with Giemsa stain. The percentage of 200 NBT-positive cells containing dark blue intracellular formazan deposits was then determined. NBT positive cells (with formazan deposits) and NBT negative cells (without formazan deposits) were counted in a total of 200 cells in each preparation, with 5 preparations for each of the groups studied. The cells were visualized using an optical microscope with an oil immersion lens (100×).

2.7. Detection of necrosis and apoptosis in HL-60 cells

Necrosis and apotosis were determined using the Apoptosis and Necrosis Quantitation Kit Plus (Quimigen). This is a convenient assay for detecting apoptotic cells (green) and necrotic cells (red) within the same cell population by fluorescence microscopy. This assay must be used on unfixed cells as the dyes included (Annexin V and EthD-III) rely on the presence of intact membranes in healthy cells to accurately distinguish healthy cells from apoptotic or necrotic cells. Prior to staining, the cells were washed with PBS and resuspended at 2–3 × 10^6 cells/mL in 1× binding buffer. The staining was carried out according to the manufacturer's instructions. Finally, the cells were covered with 1× binding buffer and the fluorescence observed using FITC and Texas Red® 3 filter sets. For each of the groups studied, necrotic and apoptotic cells were counted relative to the total number of cells in 6 fields with fluorescence microscopy at 20× magnification.

2.8. Detection of gene expression

2.8.1. mRNA extraction

After each treatment, the HL-60 cells were centrifuged at 450 ×*g* for 5 min. The L-15 culture medium was removed and the pellets were resuspended in 1 mL of TriPure reagent (Sigma-Aldrich, St. Louis, MO, USA). Chloroform (Merck, Kenilworth, NJ, USA) (0.2 mL) was added and the culture was incubated for 10 min before being centrifuged at 12000 ×*g* and 4 °C for 15 min. The phase containing the DNA, proteins and cell debris was discarded and the supernatant fraction containing the RNA was retained. The TriPure reagent residues were removed by rising the cultures with isopropyl alcohol (Merck) and 70 % ethanol (Merck) and centrifuging the culture between each wash step. The dehydrated pellet was stored at −80 °C.

Table 1
Experimental groups:

Group	Treatment
G1	HL-60 no RAD, examined at 8 or 24 h
G2A	HL-60 50 BC μg/mL + no RAD, examined at 8 or 24 h
G2B	HL-60 150 BC μg/mL + no RAD examined at 8 or 24 h
G3	HL-60 RAD 8 or 24 h
G4A	HL-60 50 BC μg/mL + RAD 8 or 24 h
G4B	HL-60 150 BC μg/mL + RAD 8 or 24 h
G5	HL-60 no RAD, examined at 48 h
G6A	HL-60 50 BC μg/mL + no RAD, examined at 48 h
G6B	HL-60 150 BC μg/mL + no RAD, examined at 48 h
G7	HL-60 RAD 48 h
G8A	HL-60 BC 50 μg/mL + RAD 48 h
G8B	HL-60 150 BC μg/mL + RAD 48 h

2.8.2. DNase treatment

The pellet was rehydrated with diethylpyrocarbonate-treated water (SigmaAldrich, St. Louis, MO) and incubated for 15 min at 60 °C. Subsequently, the RNA was quantified in a NanoDrop ND-1000 spectrophotometer (Thermo Fisher Scientific, Waltham, MA, USA). A commercial kit (Thermo Fisher Scientific, Waltham, MA, USA) containing DNase I and a reaction buffer with 2.5 mM $MgCl_2$ was used for DNase treatment. The sample was incubated with the reagents for 30 min at 37 °C, and the reaction was stopped with 50 mM EDTA from the kit.

2.8.3. RT-qPCR

The pure RNA sample (500 ng) was mixed with 1.25 μM random hexamer primers (Roche, Basel, Switzerland) and 250 μM deoxynucleoside triphosphate (dNTPs) and then incubated at 65 °C for 5 min. Reagents consisting of 200 U of reverse transcriptase (NZYtech, Portugal) in a reaction buffer of 30 mM Tris and 20 mM KCl (pH 8.3) and ribonuclease inhibitor were then added. The mixture was then placed in a thermocycler (T100™ Thermal Cycler, Bio-Rad, Watford, UK) programmed as follows: 25 °C for 10 min, 50 °C for 50 min and 85 °C for 5 min. The cDNA thus obtained from the total mRNA was then analyzed by real-time quantitative PCR (qPCR) to determine FAS-R, BCL2a and caspase-3 gene expression. The GADPH primer pair was used to normalize the data, which were expressed in relative arbitrary units (the primers used are shown in Table 3). Each sample was placed in triplicate wells of a multi-well plate (MicroAmp® Fast Optical 96 well, Life Technologies Corporation, Carlsbad, CA, USA); the first forward and reverse primers of the gene of interest were placed in the replicate wells in each case. The cDNA sample and the SYBR® Master Mix for green-based detection (Precision®-PLUS qPCR Master Mix, Camberley, UK) were also added to the wells. The cDNA was amplified using the StepOne Plus Real-Time PCR system (Applied Biosystems, Waltham, MA, USA). Apoptosis expression levels mediated via both BCL2a mitochondria-dependent regulators, and FAS-R mitochondria-independent pathways were determined and related to pre-apoptotic levels of caspase-3 at low or high doses of BC.

2.9. Detection of caspase-3/7/8 activity

2.9.1. Caspase-3/7 assay

The caspase 3/7 activity was determined using the Magic Red® Caspase-3/7 Assay Kit (ImmunoChemistry Technologies). The Magic Red® (MR) reagent is a non-cytotoxic substrate that fluoresces when cleaved by active caspase-3/7 enzymes. This enables measurement of the intracellular process of apoptosis rather than a side-effect, such as the turnover of phosphatidyl serine.

For assay, cell concentrations should be 2–8 × 10^6 cells/mL. Cells can be concentrated by lowspeed centrifugation (<200 x*g* at RT) for 5–10 min. Aliquots of at least 2 × 10^5 cells/100 μL (equivalent to 2 × 10^6 cells/mL) were transferred to each well of a black microtitre plate, taking care to prevent formation of bubbles. Staining was carried out according to the manufacturer's instructions. The fluorescence was measured at 496/520 nm (excitation/emission) in a plate fluorimeter (FLx800, Biotek).

2.9.2. Caspase-8 assay

Caspase-8 is the most upstream caspase in the CD95/Fas apoptotic pathway and is activated by the signaling pathway for CD95/Fas and TNF. The Caspase-8 IETD-R110 Fluorometric Assay Kit provides a simple assay system for fast and highly sensitive detection of caspase-8 activity.

Between 500 and 50,000 cells per well were plated in 100 uL medium in black 96-well plates. Assay buffer (100 uL) was added directly to 100 uL cells in culture medium in each well. Enzyme Substrate (Ac-IETD)2-R110 (2 mM) (5 uL) was then added and the suspension was mixed well by pipetting several times. The plates were incubated at 37 °C for 30–60 min (for a maximum of 3 h) before the fluorescence was measured at 496/520 nm (Ex/Em).

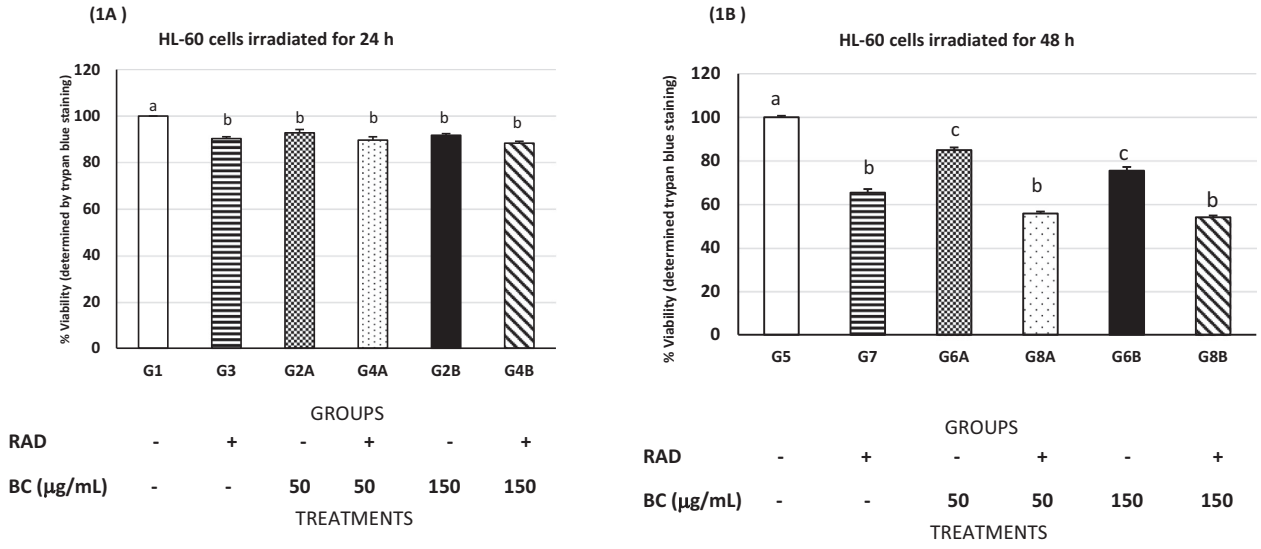

Fig. 1. Histograms showing the percentage HL-60 cell viability (determined by the trypan blue exclusion test): (A) group irradiated for 24 h, (B) group irradiated for 48 h; (A) The experimental groups are described in Table 1 and in Material & Methods section. Different letters indicate significant differences among groups ($p < 0.05$). Ninety-six samples were used, six for each group/treatment time. Mean values are shown (six samples for each group/time). Error bars indicate the standard error of the mean (SEM) within each group (irradiated with/without BC, BC only or not irradiated).

2.10. Statistical analysis

All of the values shown in the text and in the figures are expressed as means ± standard error of the mean (SEM) for each group; differences were considered significant at $p < 0.05$. Oxidative stress (reactive oxygen species) at 24 or 48 h was analyzed by two-way ANOVA. The two factors considered for the HL-60 promyelocytic cell line subjected to oxidative stress were the number of cells (healthy or damaged) and exposure to one or both environmental agents tested. The Bonferroni *t*-test for multiple comparisons was subsequently used to detect between -group differences. Viability, necrosis and apoptosis, expression of the BCL2a, FASR and caspase-3 genes and intracellular activity of caspase 3 and caspase 8 were analyzed by one-way ANOVA and a post hoc Tukey test for multiple comparisons. The data were transformed using natural logarithm transformations when they did not meet the assumptions of normality and homoscedasticity. All statistical analyses were performed with Sigma Plot 14.0 (Systat Software Inc., San Jose, CA, USA) and Grath Pad InStat. Culture data were obtained from at least four separate experiments and the values were normalized relative to the control group values (100 %).

3. Results

3.1. Analysis of cell viability

The results indicated important alterations in the viability and proliferation of HL-60 cells due to the combined effect of irradiation and BC exposure. Statistical analysis of cell viability by groups provided the following information:

HL-60 cells in all groups examined after irradiation for 24 h showed a significant decrease in cell viability ($p < 0.001$, in all cases), especially G3 (90.2 ± 0.8 %), along with G4A (89.6 ± 1.4 %) and G4B (88.3 ± 0.8 %), which were exposed to radiation and black carbon (BC). There was also a significant decrease, although to a lesser degree, in the viability of HL-60 cells in G2A, exposed to BC (92.7 ± 1.4 %), and G2B (91.7 ± 0.7 %), not irradiated ($p < 0.001$, in all cases) (Fig. 1A).

When the irradiation time was increased to 48 h, HL-60 viability decreased drastically in all groups, to 55.7 ± 0.8 % in G8A (HL-60 50 BC μg/mL + RAD 48 h), to 65.3 ± 1.6 % in G7 (the HL-60-RAD 48 h) and 84.8 ± 1.2 % in G6A (HL60-50 BC μg/mL + no RAD 48 h) relative to G5, (HL60 no RAD 48 h) ($p < 0.001$, in all cases) (Fig. 1B).

The combined effect of HL-60-150 BC μg/mL + RAD 48 h in G8B caused intense toxicity, decreasing cell viability by up to 54 ± 0.8 % relative to G5 (the HL-60 no RAD 48 h) ($p < 0.001$). Cell viability also declined significantly to 75.4 ± 1.7 % in G6B (HL-60 -150 BC μg/mL + no RAD 48 h) and to 65.32 ± 1.6 % in G7 (HL-60 RAD 48 h) relative to G5 (the HL-60 no RAD 48 h) ($p < 0.001$ in both cases) (Fig. 1B).

3.2. Antiproliferative effects

Results for antiproliferation or cell growth inhibition after 24 or 48 h of irradiation are shown in Tables 4 and 5.

3.3. Nitroblue tetrazolium (NBT) assay

Twenty-four hours after irradiation, the NBT assay, used to measure ROS production in the cells, revealed increased levels of damage or no damage, depending on the level of irradiation or exposure to BC alone or the combination of BC and irradiation. Statistically significant interactions between the health status of cells (damaged/ health) and irradiation or exposure to BC alone or the combination of both ($p = <0{,}001$).

Multiple comparisons were made between the groups and the non-irradiated control group cell cultures examined after 24 h (Holm-Sidak method), with an overall significance $p < 0.05$.

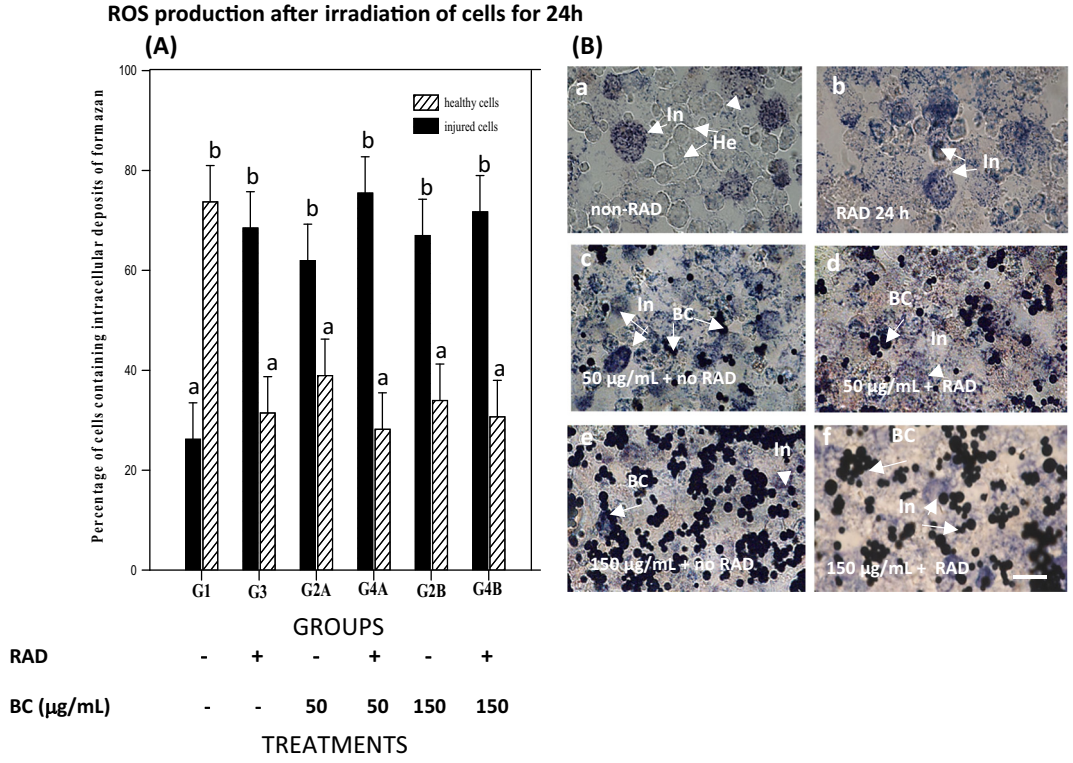

Fig. 2. (A). Histograms showing the percentage of HL-60 cells containing intracellular formazan deposits used to determine ROS production in groups irradiated for 24 h. The experimental groups are described in Table 1 and in Material & Methods. Different letters indicate significant differences among groups ($p < 0.05$). One hundred cells were counted in each of six samples for each group. Error indicates the standard error of the mean (SEM) within each group (radiated with/without BC, only BC or not irradiated). **(B)** Microphotographs showing ROS levels and oxidative stress effects in HL-60 cells, measured with the nitroblue tetrazolium (NBT) assay, after exposure to 2.45 GHz RF radiation and BC particles. In the photograph, healthy cells (He), damaged cells (In) and black carbon (BC) particles are indicated by white arrows. Calibration bar, 10 μm.

Comparison of damaged cells from each treated group and G1 (the non-irradiated control group), revealed significant differences in all cases ($p < 0.001$). However, in multiple comparisons regarding healthy cells, significant differences were also observed between the different groups and G1 ($p < 0.001$), except for G2A (HL-60 50 BC μg/mL + no RAD 24 h), in which the difference was significant at $p = 0.02$.

Oxidative stress levels, measured as ROS production, increased in relation to irradiation (24 h), BC level and the combination of both. Significant differences were observed between injured and healthy cells in all groups ($p < 0.001$ in all cases), except for G2A (HL-60 50 BC μg/mL + no RAD 24 h) ($p = 0.03$) and G2B (150 μg/mL + no RAD 24 h) ($p = 0.003$) (Figs. 2A and 2B).

In the cells irradiated for 48 h, the results of the NBT assay revealed sustained damage to the cells. This was reflected in the ratios of damaged and healthy cells, depending on the radiation level, exposure to BC alone or the combination of both. There was a statistically significant interaction between proportion of damaged/healthy cells, irradiation and exposure to BC alone or in combination ($p < 0.001$).

Multiple comparisons were made after 48 h between the treatment groups (G2A to G8B) and the non-irradiated control group (G1) (Holm-Sidak method), with a global significance level of 0.05. Significant differences were also found for damaged cells in all relevant groups relative to G1 ($p < 0.001$). Multiple comparisons relative to healthy cells also revealed significant differences between the treatment groups and the non-irradiated control cells in G1 ($p < 0.001$).

Oxidative stress or ROS production increased with irradiation time (48 h), BC level and the combination of both. Significant differences between damaged cells and healthy cells were observed in all groups ($p < 0.001$ in all cases), except for G2A (HL-60 50 BC μg/mL + no RAD 48 h) ($p = 0.018$) (Figs. 3A and 3B).

Table 2
Experimental conditions of the groups exposed to RF radiation.

Mean SAR (W/kg)				
f (MHz)	PTR (W)	Em (V/m)	PD (W/m ^{2})	Culture flasks
2450	12	102.8	28	0.4060

3.4. Cell death: Necrotic or/and apoptotic HL-60 cells

Analysis of the data indicated that 24 h irradiation had a significantly weaker effect than that BC in relation to triggering cell necrosis. Thus, the groups in which the highest levels of necrosis were observed relative to G1 and G3 were the non-irradiated groups, G2A (Hl-60 50 BC μgr/mL + no RAD 24 h) (32 % ± 2) and G2B (Hl-60 150 BC μgr/mL + no RAD 24 h) (38 % ± 1.4) ($p < 0.001$ for both). However, the levels of necrosis in the irradiated groups G4A (HL-60 50 BC μg/mL + RAD 24 h) and G4B (Hl-60 150 BC μg/mL + RAD 24 h) were not significantly higher than in G1 but <25 % (in both $p < 0.05$; $p < 0.01$). In addition, in G3 (Hl-60 RAD 24 h), in which the HL-60 cells were only irradiated for 24 h, no significant differences were observed relative to G1 ($p > 0.05$) (Fig. 4 A1).

After irradiation for 24 h, apoptosis was modulated in the cells exposed to 50 μgr BC, and the percentage of apoptotic cells (24 % ± 2) was only significantly higher in G4A (HL-60 50 BC μg + RAD 24 h) than in G1 ($p < 0.01$). However, in the group of HL-60 cells that were not irradiated but exposed to 50 μg BC, G2A, the level of apoptotic cells was not significant ($p > 0.05$) relative to G1, which already had a high level of necrotic cells (32 % ± 2). In the other groups, when the cells are subjected to the highest dose of BC (150μgr) with or without radiation (G2B and G4B) the

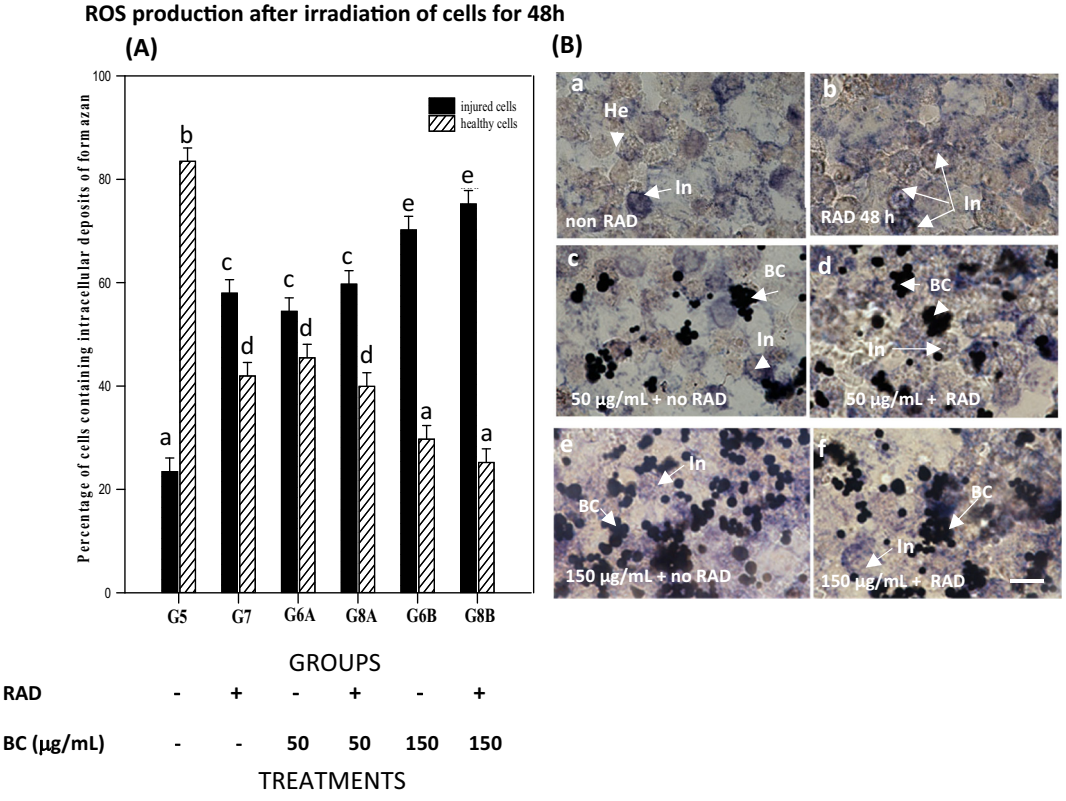

Fig. 3. (A). Histograms showing the percentage of cells containing intracellular formazan deposits indicating ROS production in groups irradiated for 48 h. The experimental groups are described in Table 1 and in Material & Methods.Different letters indicate significant differences among groups ($p < 0.05$). One hundred cells per six samples were used, six for each group. Mean values are shown (six samples for each group/treatment time). Error bars indicate the standard error of the mean (SEM) within each group (radiated with/without BC, only BC or not irradiated). **(B)** Microphotographs showing ROS levels and oxidative stress effects in HL-60 cells, measured with the nitroblue tetrazolium (NBT) assay, forty-eight hours after exposure to 2.45 GHz radio frequency electromagnetic fields and BC particles. In the photographs, healthy cells (He), damaged cells (In) and black carbon (BC) particles are indicated in white. Calibration bar 10 μm.

Table 3
Primer sequences used for reverse transcription quantitative polymerase chain reaction (RT-qPCR).

	Primer	Accession number	Forward sequence (5′-3′)	Reverse sequence (5′-3′)
Human	GADPH		GCCTCACTCCTTTTGCAGAC	TTCTAGACGGCAGGTCAGGT
	BCL2a	NM_000633.3	TGCGGCCTCTGTTTGATTTC	ATTTGTTTGGGGCAGGCATG
	FASR	NM_000043.6	TCAGTACGGAGTTGGGGAAG	CAGGCCTTCCAAGTTCTGAG
	CASP3	NM_004346.4	TTTTTCAGAGGGGATCGTTG	CGGCCTCCACTGGTATTTTA

percentage of apoptotic cells was not significant ($p > 0.05$), relative to cells than were only irradiated (G3) (Fig. 4 A2).

Irradiation of the HL-60 cells for 48 h triggered high levels of cell death. The high dose of BC alone, with no irradiation induced very high levels of necrosis in G2B (39 % ± 2.4), which were significantly higher than in G5 ($p < 0.001$). Likewise, the lower dose of BC without radiation also induced a significantly higher level of necrosis in G2A (24 % ± 3.5) than in G5 ($p < 0.05$). Irradiation alone induced a high percentage of necrosis in G7 (36% ± 4) and was significantly higher ($p < 0.001$) than in the non-irradiated G5. On the other hand, the combined exposure of both the irradiation and the maximum dose of BC in G8B induced similar levels of necrosis (36 % ± 5) to that in G7 (36% ± 5) and was statistically significantly higher ($p < 0.001$) than in G5 (Fig. 4 A1). The combination of a low dose of BC and irradiation for 48 led to a significantly higher level of necrosis in G8A than in G5 ($p < 0.05$) (Fig. 4 A1).

After 48 h irradiation, the combined effect of irradiation and low doses BC induced significantly higher levels of apoptosis in G8A (29 % ± 4) than in G5 ($p < 0.05$). In addition, the levels of apoptosis induced by the combined effect of irradiation and 50 BC μgr in G8A were significantly higher ($p < 0.05$) than induced by the action of high doses of BC alone (G6B) (150 μg/mL /mL + no RAD 48 h). (See Fig. 4 A2). The effect of 48 h irradiation (G7) also induced significantly higher levels of apoptosis (23 % ± 2) than in G5 ($p < 0.05$).

In the other groups, the levels of apoptosis induced by the combination of irradiation and BC, or by the BC alone were not significantly higher than in G5 ($p > 0.05$).

3.5. Individual and combined effects of RF radiation and black carbon

3.5.1. Effect on BCL-2a gene expression in the mitochondria-dependent pathway

After 24 h irradiation, the action of RF or BC particles significantly increased the BCL-2a values in G2A (1.29 ± 0.054), G2B (1.32 ± 0.023) and G3 (1.33 ± 0.05) relative to G1 0.99 ± 0.034) ($p < 0.05$ in all cases) (Fig. 5A).

However, in G4A (1.06 ± 0.07) and G4B (1.01 ± 0.12), the values were not significantly higher than in G1 ($p > 0.05$). It is important to note that 24 h irradiation alone induced a significantly greater increase ($p < 0.05$) in the antioxidant activity of the BCL2a protein than the combined action to G4B (Fig. 5A).

After 48 h irradiation, there were no significant differences ($p > 0.05$) in any of the groups relative to G5 (Fig. 5B).

3.5.2. Effect on FAS-R gene expression: Involvement of an extrinsic pathway

None of the HL-60 cell groups subjected to the combination of irradiation and BC (50 or 150 μg /mL) or to each treatment only showed significant differences in FAS-R values relative to G3.

After 48 h irradiation, the combined action of RF and BC particles significantly increased FAS-R values in G8A (1.32 ± 0.086) and G7 (1.45 ± 0.47) relative to G5 (1.01 ± 0.07) ($p < 0.05$ in all cases) (Fig. 6A).

There were no significant differences ($p > 0.05$) in FAS-R expression in any of the other irradiated groups, G8B or G8A, or non-irradiated groups, G6A, G6B, relative to the control G5 (Fig. 6B).

3.5.3. Effects on caspase-3 activity

Twenty-four hours after treatment, there were no significant differences ($p > 0.05$) in caspase-3 activity in any of the treated groups relative to the control group (G1.

Forty-eight hours after treatment, the cells irradiated for 48 h, i.e. G7 ($p < 0.01$) and G8A, showed significant differences ($p < 0.05$) compared to G5 (Fig. 7).

3.6. Effect on apoptosis over time as measured by intracellular caspase activity in HL-60 cells

3.6.1. Caspase-3 activity

Determining caspase 3 activity in the cells eight hours after irradiation enabled detection of the levels of early apoptosis in Hl-60 promyelocytic cells. Intense caspase 3 activity was observed for both eight hours of irradiation only and BC exposure only on HL-60 cells. In the group that only exposed to radiation (G7) the difference in levels of early apoptotic activity of caspase 3 and/or 7 (27,108.5 ± 1822) relative to the non-irradiated G5 were highly significant ($p < 0.001$). Likewise, the maximum dose of BC (150μg) alone (G2B) caused highly significant levels of caspase-3 and -7 activity (22.000 ± 2400) ($p < 0.001$) relative to the non-irradiated group (G5). Similarly, the combined effect of eight hours of irradiation and exposure to 50μg BC caused a significant increase ($p < 0.001$) in early apoptotic activity, although in group G4A the levels of caspase-3 and -7 (19,892 ± 1581) did not exceed those induced by irradiation or BC alone. The caspase 3 activity was not significantly higher in G2A and G4B ($p > 0.05$) than in G1 (Fig. 8).

Twenty-four hours after continued irradiation or BC exposure, caspase 3 activity was significantly elevated only in the groups of cells exposed to doses of 50 ($p < 0.01$) and/or 150 μg ($p < 0.01$) of BC, without irradiation (G2A or G2B), relative to non-irradiated cells (G1) or irradiated cells (G3) ($p < 0.01$). The antioxidant action was very effective in the group irradiated for 24 h (G3), so there were no significant differences in caspase 3 activity relative to the non-irradiated group (see results 3.5.1 and Fig. 5). There were also no significant differences between the groups treated by the combination of irradiation and 50 or 150 μg BC for 24 h (G4A or G4B). Black carbon was also found to counteract the caspase 3 machinery, as indicated by the significantly low values relative to G2A ($p < 0.001$) and G2B ($p < 0.01$) (Fig. 8).

Forty-eight hours after treatment, caspase-3 activity was highest in G7 (15,690 ± 510), irradiated for 48 h, and significantly higher than in G1 ($p < 0.05$). This group (G7) also presented significant differences relative to the groups subjected to the combined effects of BC and radiation: G8A (50 BC μg/mL + RAD) and G8B (150 BC μg/mL + RAD) ($p < 0.01$). However, there were no significant differences between the other groups, except G7 and G5 (Fig. 8).

Table 4
Inhibition of cell growth after irradiation for 24 h relative to the control group (G1).

	Groups				
Percentage inhibition of cell growth at 24 h	G3 4.46 %	G2A 1.46 %	G4A 5.46 %	G2B 2.46 %	G4B 6.46 %

Table 5
Inhibition of cell growth after irradiation for 48 h relative to the control group (G5).

	Groups				
Percentage inhibition of cell growth at 48 h	G7 25.95 %	G6A 2.95 %	G8A 37.95 %	G6B 13.95 %	G8B 39.95 %

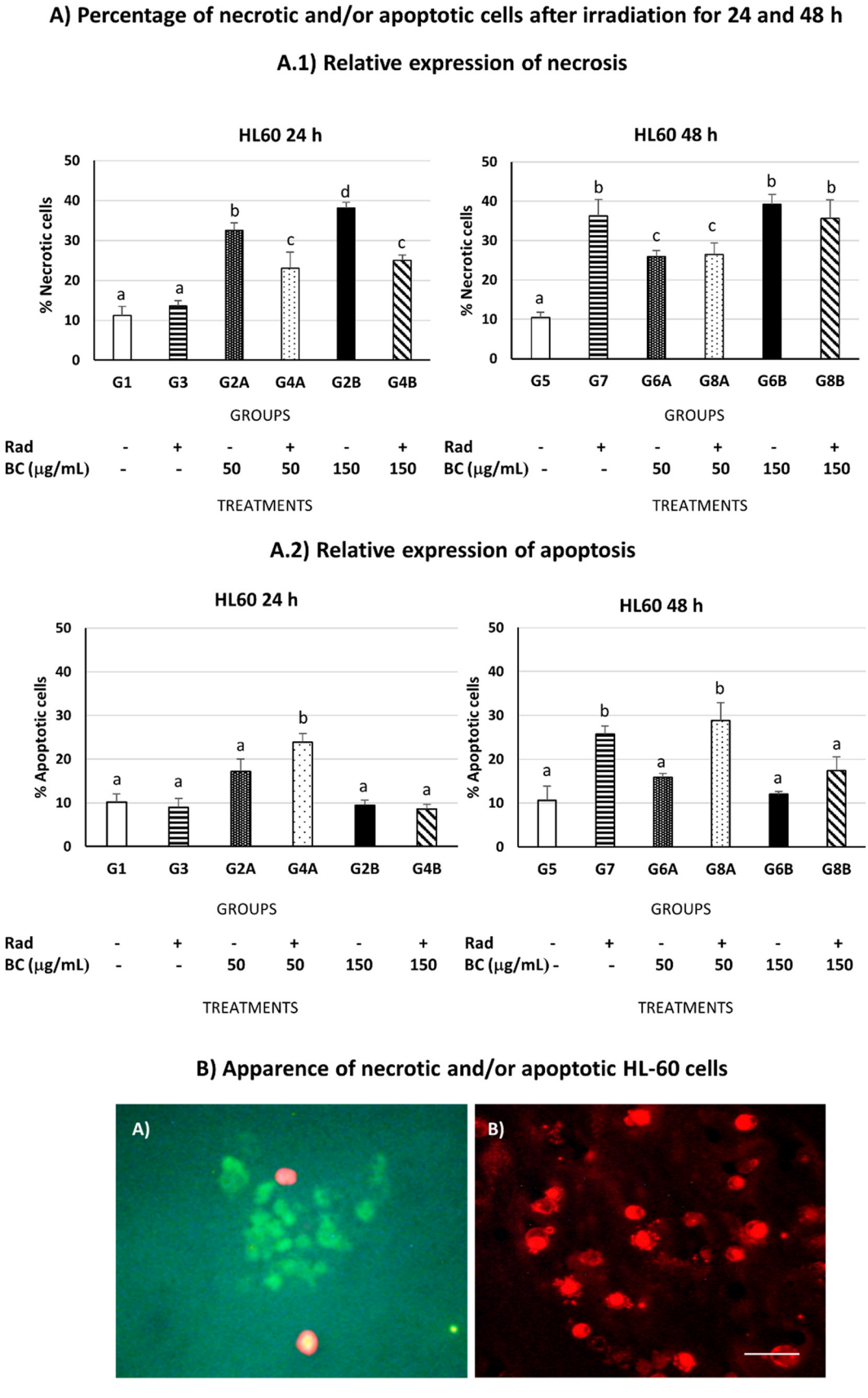

Fig. 4. (A). Histograms showing the percentage of necrotic (A1) and/or apoptotic (A2) HL-60 cells after irradiation for 24 and 48 h. The experimental groups are described in Table 1 and in Material & Methods. Different letters indicate significant differences among groups ($p < 0.05$). (B) Fluorescence microphotographs showing (A) HL-60 non-RAD 24 h with apoptotic green cells and necrotic red cells (B) HL-60 150 BC μg/mL + no RAD 24 h with necrotic red cell. Necrotic and apoptotic cells were counted relative to the total number of cells in 6 fields at 20 × magnification for each group. Error bars indicate the standard error of the mean (SEM) within each group (irradiated with/without BC, only BC or not irradiated). Scale bar = 20 μm.

3.6.2. Caspase-8 activity

After irradiation of the samples for 8 h, the caspase 8 levels were higher in the group of non-irradiated HL-60 cells than in the groups that were irradiated and/or exposed to BC. No caspase 8 activity was observed in any of the groups exposed to different doses of BC or after combined exposure of BC and irradiation.

Similarly, after 24 or 48 h, caspase 8 levels were not significantly higher than in the non-irradiated group. No significant activity of this enzyme was detected in any of the irradiated or non-irradiated groups studied, whether exposed or not to doses of BC 50 or 150 μg/mL (see Fig. 9 A, B and C).

4. Discussion

Our experimental results indicate that the combined effect of exposure to non-ionizing 2.45 GHz radiation and black carbon (BC) provoked high levels of cytotoxicity in the HL-60 human myeloid cell line. The cytotoxicity was reflected as relatively high levels of early apoptosis and necrosis and anti-proliferative effects associated with the ROS production, detected as early as 24 h after exposure and maintained for at least 48 h. The oxidative stress metabolism triggered by external stressors interacting with the promyelocytic cells activated gene expression of the anti-apoptotic mitochondrial BCL2a after 24 h irradiation and exposure to BC. We have also experimentally demonstrated the early damaging effect, 8 h after exposure to radiation or BC, triggering the activation of caspase-dependent apoptosis in the HL-60 promyelocytic cell line by mitochondrial damage. The persistent activation of caspase-3 after 48 h irradiation confirmed the involvement of the mitochondrial machinery through the intracellular intrinsic pathway. However, there was no evidence that the extrinsic pathway of apoptosis is activated by elevation of expression of the FAS-R cell death receptor, as this was not accompanied by a significant increase in caspase 8 levels.

High levels of damage in the HL-60 cells from the combined interaction of both environmental pollutants has been found to provoke alterations in reticulocyte function. This is associated with impairment of antimicrobial action (Kobayashi et al., 2017), creating a microenvironment in which inflammatory (Rebuli et al., 2021) or autoimmune (Noorimotlagh et al., 2021) dysfunctions may appear.

The survival of the promyelocytes obtained from this cell line after exposure to radiofrequency electromagnetic fields was related to the electromagnetic parameters of frequency, power and exposure time (García-Minguillán López et al., 2019;Vagdatli et al., 2014). Previous research involving exposure of the HL-60 cell line to non-thermal 2.45 GHz RF radiation also showed a significant reduction in cell viability (Asano et al., 2017a and b; Lee et al., 2005). However, our experimental findings of anti-proliferation (Tables 4 and 5) contrast with those of Nazıroğlu et al. (2012), who reported increased cellular proliferation when the exposure involved power of <2 W. This leads us to think that the EMF exposure parameters applied determined the biological effect and were decisive for promyelocyte cell survival (Di et al., 2018; Lippi et al., 2016; Koyama et al., 2015). Accordingly, the anti-proliferative effects of EMFs in cells and/or tissues may potentially modulate cell growth and reverse pathological states such as cancer (López-Martín et al., 2021; Barati et al., 2021).

No alterations in HL-60 cell viability have been found at other frequencies (Koyama et al., 2015), including 900 MHz (Sun et al., 2017). However, the effect of non-ionizing radiation on the viability of this promyelocytic cell line has generated controversy and discussion among researchers (Speit et al., 2013; Adlkofer, 2014). Exposure time constitutes an important factor in HL-60 cell viability and our findings are consistent with those obtained by other authors (Asano et al., 2017a), as HL-60 cell survival decreased substantially as the irradiation time increased from 24 to 48 h. While the EMF parameters established in the irradiation system were crucial for obtaining these experimental results, the HL-60 promyelocytic cell line chosen and the in vitro exposure model were equally important. In recent normothermic exposure studies of 8 cell lines exposed to 2.45 GHz RF, the HL-60 promyelocytic cell line showed the greatest vulnerability, and non-ionizing radiation considerably diminished the cell viability (Asano et al., 2017b).

Damage to this cell line also appeared with exposure to environmental particles only, as described by other authors (Wang et al., 2020). We observed a significant but moderate, decrease in neutrophil precursor cell survival after 24 h exposure to BC, in contrast to the findings of other authors who reported maximum levels of neutrophil cell death for the same exposure time (Wang et al., 2020). Thus, the percentage cell necrosis induced by the effect of BC only reached between 33 % and 38 % depending on the dose (Fig. 4 A1), and the level of necrosis reached by the combined action of BC and radiation was much lower, around 24 %. Thus, although the combined action of both radiation and BC appeared after 24 h, the damaging effect of radiation occurred later, thus delaying cell death caused by BC.

In the present study, the maximum decrease in cell survival appeared at 48 h (Fig. 1A,B) and was depended on BC concentration (Ahmad et al., 2015). Thus, the maximum expression of cell death was observed in this experiment, with levels of necrosis close to 40 % caused by exposure to the maximum dose of BC (150 μg) and/or the combined action of BC and radiation and/or the effect of 48 h irradiation only. Thus, the toxic effect of radiation on the HL-60 cells was much more evident after 48 h irradiation, alone or in combination with BC, so that radiation potentiates the effect of BC (Figs. 4 A1 and Figs. 4 A2). Secondly, a period of 48 h was also necessary for the maximum apoptotic activity to appear due to the combined effect of radiation and BC 50 μgr (Fig. 4 A1). The synergic action of the two environmental stressors (RF radiation and suspended BC particles) (Sueiro-Benavides et al., 2021) caused important bioeffects in HL-60 promyelocytic cells at 48 h. Both individually and in combination, they impaired cellular functioning and diminished cell viability by as much as 54.1 %.

Calcium ions are involved in maintaining a balance between cell survival and cell death. They may even control cell viability as they act as ubiquitous second messengers that can regulate many intra- and inter-cellular responses to diverse stress agents (Wójcik-Piotrowicz et al., 2016). Some physical models assume that non-ionizing radiation (as a stress factor) generates mechanisms that alter ionic transport and/or lead to dysfunction in ion-protein complexes (Wojcik-Piotrowicz et al., 2017; Wócik-Piotrowicz et al., 2014) through an imbalance in the calcium-dependent signaling pathway (Pilla et al., 2011). However, BC proved highly toxic to promyelocytic cells after exposure for 48 h and decreased the cell viability to 75 %.

This finding is consistent with those of other in vitro experimental studies involving mitochondrial dysfunction with alteration of the Ca^{2+} channels (Shang et al., 2021, Westphal et al., 2015; Faizan and Ahmad, 2021. The decreased levels of cell survival levels observed in the present study indicate a toxic synergic effect (Kostoff and Lau, 2017) and confirm the high sensitivity of the HL-60 cell line to radiation (Asano et al., 2017a) and environmental particles (Wang et al., 2020).

This experimental study produced evidence of high levels of oxidative stress in the HL-60 human promyelocytic cell line after 24 h exposure to 2.45 GHz RF radiation or exposure to BC, as described by respectively Nazıroğlu et al. (2012) and Johnston et al. (2015). However, we have shown, for the first time, this effect for combined exposure to both environmental stressors (Figs. 2 and 3). Use of the NBT assay to assess the effects of oxidative cellular metabolism and/or oxidative stress levels enabled qualitative and quantitative determination of ROS production, which is directly related to levels of formazan crystals in the cellular cytoplasm (Esfandiari et al., 2003; Choi et al., 2006). Other authors have described how moderate levels of oxidative stress increased cellular differentiation in neutrophils (Nazıroğlu et al., 2012; Hu et al., 2014) but high levels of oxidative stress provoked inhibition of cellular proliferation and toxicity (Johnston et al., 2015). In the present study, high levels of oxidative stress were also reached and maintained after 48 h irradiation. The anti-proliferative effect (Barati et al., 2021) reached maximal levels in the promyelocytic cell line (Table 2) in response to the combination of both RF radiation and BC. Cell growth was inhibited by 37.95 % in the group exposed to the lower dose of BC and irradiated for 48 h and 39.95 % in the group exposed to the higher dose of BC and irradiated for 48 h. These high levels of oxidative stress triggered the production of antioxidant mechanisms at the cellular level (Su et al., 2019). The resulting balance of both systems determined the degree of oxidative damage and cellular dysfunction (Kovacic and Somanathan, 2010, 2008).

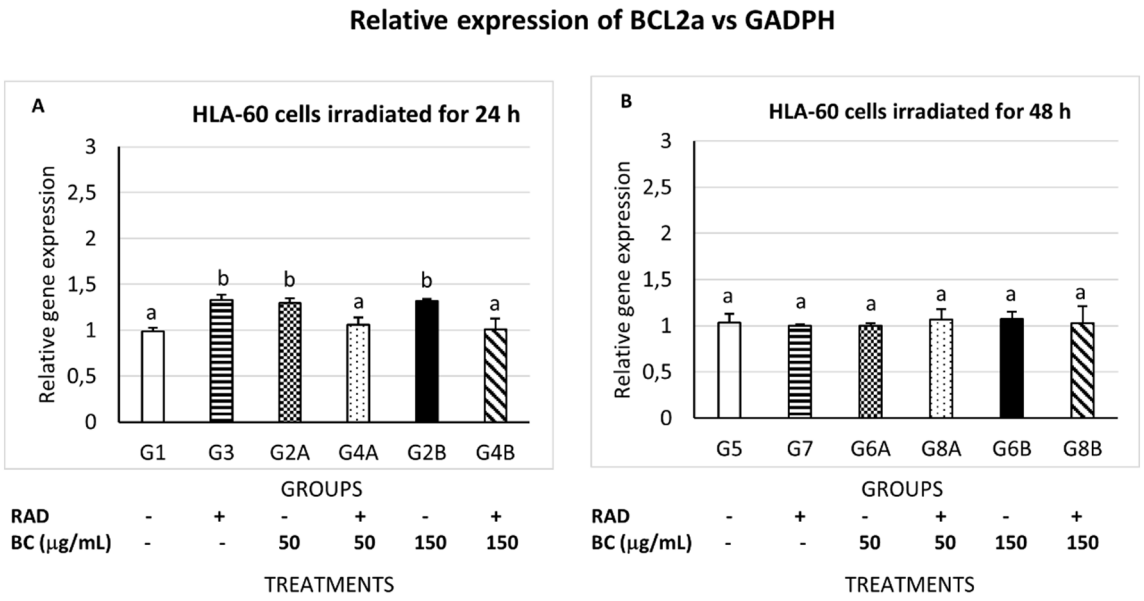

Fig. 5. Histograms of mRNA BCL2a gene expression: (5A) HL-60 cells irradiated for 24 h. (5B). HL-60 cells irradiated for 48 h. The experimental groups are described in Table 1 and in Material & Methods. The values shown are means (six samples for each group/time). Bars indicate the standard error of the mean (SEM) within each group (irradiated with/without BC, only BC or not irradiated). Different letters indicate significant differences among groups ($p < 0.05$).

This study also revealed a strong correlation between the intra-cellular effects of ROS and/or the negative effects on cellular viability in the promyelocytic line: these effects were dose-dependent for the BC particles (Sarkar et al., 2011). The oxidative response increased in tandem with the BC dose, especially in the first 24 h (Fig. 2A, B) (Johnston et al., 2015). After 48 h exposure to BC, oxidative stress (Fig. 3A, B) and cytotoxicity reached their highest level (Fig. 1B) and can be attributed to the very high levels of cellular death in the intracellular machinery (Sueiro-Benavides et al., 2021).

Studies with diverse in vivo and in vitro models have indicated that environmental interactions between electromagnetic fields and live matter can provoke oxidative stress and generate an antioxidant response and mitochondrial imbalance. This depends on EMF intensity, frequency and exposure time and the particular cell lines and tissues (Schuermann and Mevissen, 2021; Santini et al., 2018). In the present study, radiation alone generated cellular oxidative stress and increased inhibition of HL-60 cell proliferation by 20 % between 24 and 48 h after RF exposure (Figs. 2, 3A and B).

The need for objective scientific studies to investigate whether RF fields can induce oxidative stress in various types of cells and therefore damage human and animal health has led the WHO to commission expert researchers to establish oxidative stress biomarkers using systematic study protocols (Henschenmacher et al., 2022). The findings of the present study could be included in the systematic classification as they provide biomarkers for quantifying altered redox homeostasis (intracytoplasmic ROS measured by NBT) after exposure to RF EMF at 2.45 GHz (see all electromagnetic parameters in Methodology, Table 3) and non-thermal SAR in

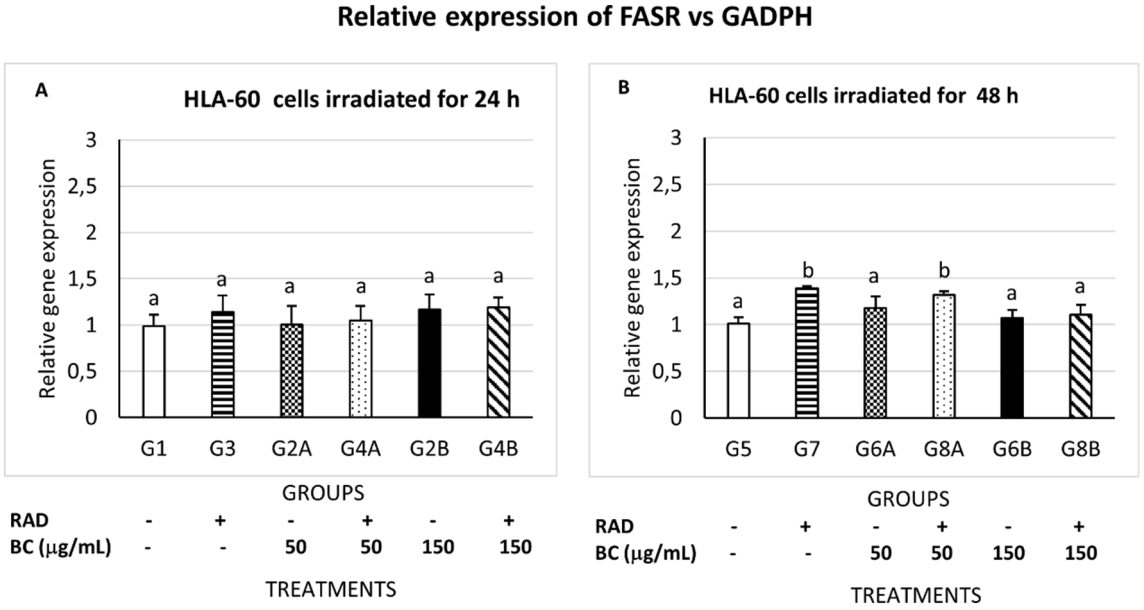

Fig. 6. Histograms of mRNA FASR gene expression: (6A) HL-60 irradiated for 24 h. (6B) HL-60 irradiated for 48 h. The experimental groups are described in Table 1 and in Material & Methods. The values shown are means (six samples for each group/time). Error bars indicate the standard error of the mean (SEM) within each group (irradiated with/without BC, only BC or not irradiated). Different letters indicate significant differences among groups ($p < 0.05$).

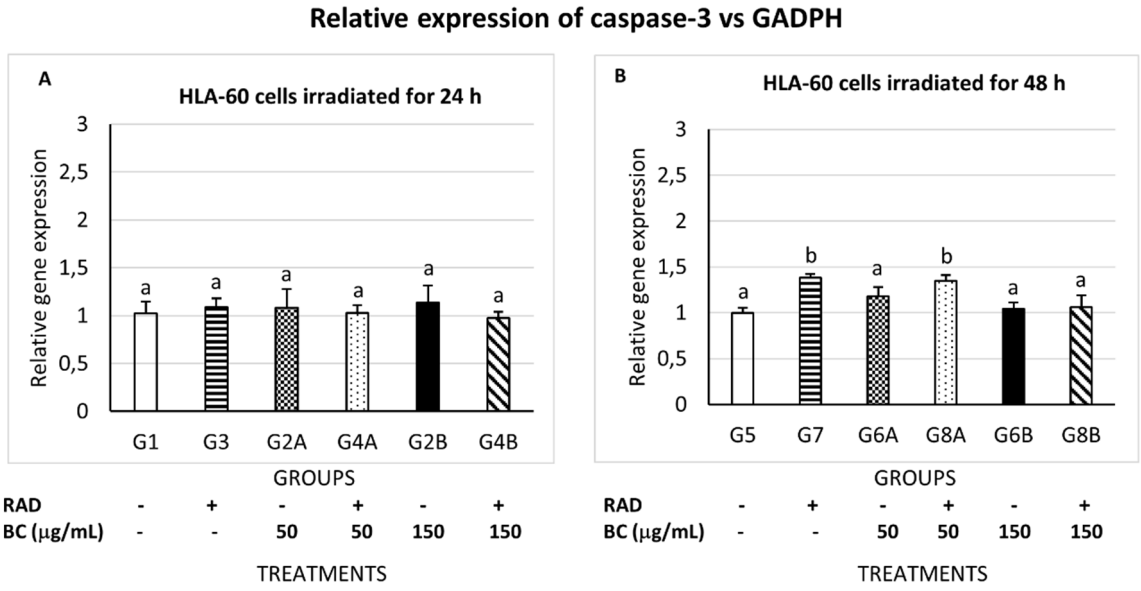

Fig. 7. Histograms of mRNA caspase-3 gene expression (7A); HL-60 irradiated for 24 h (7B). The experimental groups are described in Table 1 and in Material & Methods. The values shown are means (six samples for each group/time). Bars indicate the standard error of the mean (SEM) within each group (irradiated with/without BC, only BC or not irradiated). Different letters indicate significant differences among groups ($p < 0.05$).

an in vitro model of promyelocytic cells (see also Nazıroğlu et al., 2012; Sun et al., 2017). The high levels of oxidative stress associated with BC and RF observed in the present in vitro study suggest that an environmental context where both stressors occur together may facilitate or accelerate mechanisms that lead to inflammatory response, cell injury and diverse pathologies in living beings (Salas-Sánchez et al., 2019; Rao et al., 2018). Due to

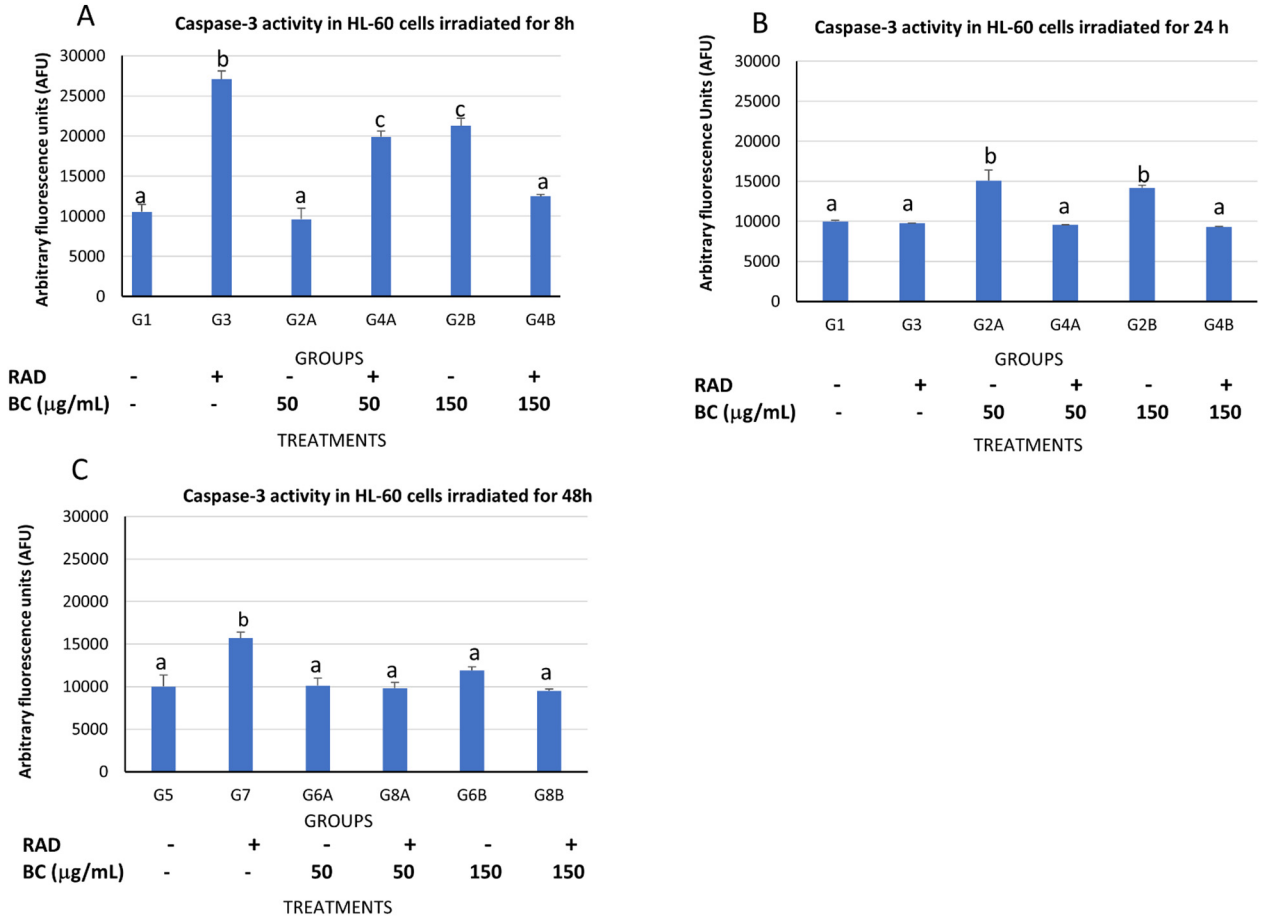

Fig. 8. Histograms showing intracellular activity caspase-3: (A) HL-60 irradiated for 8 h. (B) HL-60 irradiated for 24 h (C) HL-60 irradiated for 48 h. The experimental groups are described in Table 1 and in Material & Methods. The values shown are means (six samples for each group/time). Bars indicate the standard error of the mean (SEM) within each group (irradiated with/without BC, only BC or not irradiated). Different letters indicate significant differences among groups ($p < 0.05$).

the dramatic decrease in cell viability and high toxicity that appeared 48 h after the continuous action of one or both environmental stressors, i.e. RF radiation (Asano et al., 2017b) and/or environmental particulate matter (Sarkar et al., 2011), we deduce that mechanisms which cause irreparable damage to HL-60 cells are activated. Overproduction of ROS, which was already detected at very high levels after 24 h (Fig. 2A, B), could damage DNA in the mitochondria or nucleus and induce a cascade of pathways that activate gene transcription. These genes would change the pathways regulating cell survival and eventually cause cytotoxicity and apoptosis (Chu et al., 2021). Thus, we explored whether oxidative stress from RF and BC activated programmed cell death or apoptosis and whether it was mediated by a mitochondria-dependent pathway or an independent external pathway (Palumbo et al., 2006; Reed, 2000).

Our findings indicate that the environmental stressors (radiation and BC) acted both separately and together by triggering apoptosis in a programmed way through mitochondrial dysfunction and possibly by stimulating expression of cell death receptors (González et al., 2010; Danial and Korsmeyer, 2004). Examination of each of the experimental events showed that the process was initiated 24 h after exposure to RF radiation (Asano et al., 2017b) and/or BC particles (de Almeida Rodolpho et al., 2021) and led to a significant increase in the expression of the anti-apoptotic protein BCl-2a in G3 (HL-60 RAD 24 h), G2A(HL-60 50 BC μg/mL + no RAD 24 h) and G2B (HL-60 150 BC μg/mL + no RAD 24 h) (Fig. 4). The antioxidant action did not occur in response to combined exposure to RF and BC, probably because other cell-damaging mechanisms were activated in the cell (Barati et al., 2021). The BCL-2a family regulates the membrane potential and permeabilization of the mitochondrial membrane (Danial, 2007), which is dependent on the positive charge of calcium in human HL-60 promyelocytic cells (Zhang et al., 2000; González et al., 2010). Both external pollutants created elements that oxidised various phospholipids in the cell membrane (Kagan et al., 2000) and later blocked oxidation and apoptosis via the BCL-2a anti-apoptotic protein (Fabisiak et al., 1997). This antioxidant and anti-apoptotic mechanism occurs in response to oxidative stress and is mediated by the mitochondria-dependent pathway (Keeble and Gilmore, 2007; Shang et al., 2021). The antioxidant response was not accompanied by a lack of activation of the FAS (CD95) receptors or cell death receptors in any of the experimental groups exposed to radiation or BC (Fig. 5A) (Danial and Korsmeyer, 2004). This external receptor in the promyelocytic cell membrane belongs to the TNF family (Magnusson and Vaux, 2000) and seems to be linked to the production of apoptosis caused by oxidative stress signals (Kagan et al., 2000) that are considered important for resolving cell death. During this time there was no enzymatic activation of caspases in the mitochondrial pathway (Youle and Strasser, 2008; Danial, 2007), by activation of cellular death receptors or by an extrinsic pathway (Ashkenazi and Dixit, 1998). This was reflected in the non-significant expression of caspase-3 in some of the experimental groups after 24 h (Fig. 7A). However, caspase-3 activity was significantly higher in the group exposed to the lower dose of 50 BC μg/mL and irradiated for 8 or 24 h than in the non-irradiated control group. After 24 h, high levels of cell necrosis were observed in both groups exposed to either of the BC doses (G2A and G2B) or with combined exposure to radiation and BC (G4A and G4B) (Fig. 4 A1).

Forty-eight hours after irradiation and BC exposure, we observed activation of the FAS cellular death receptors, which were expressed at

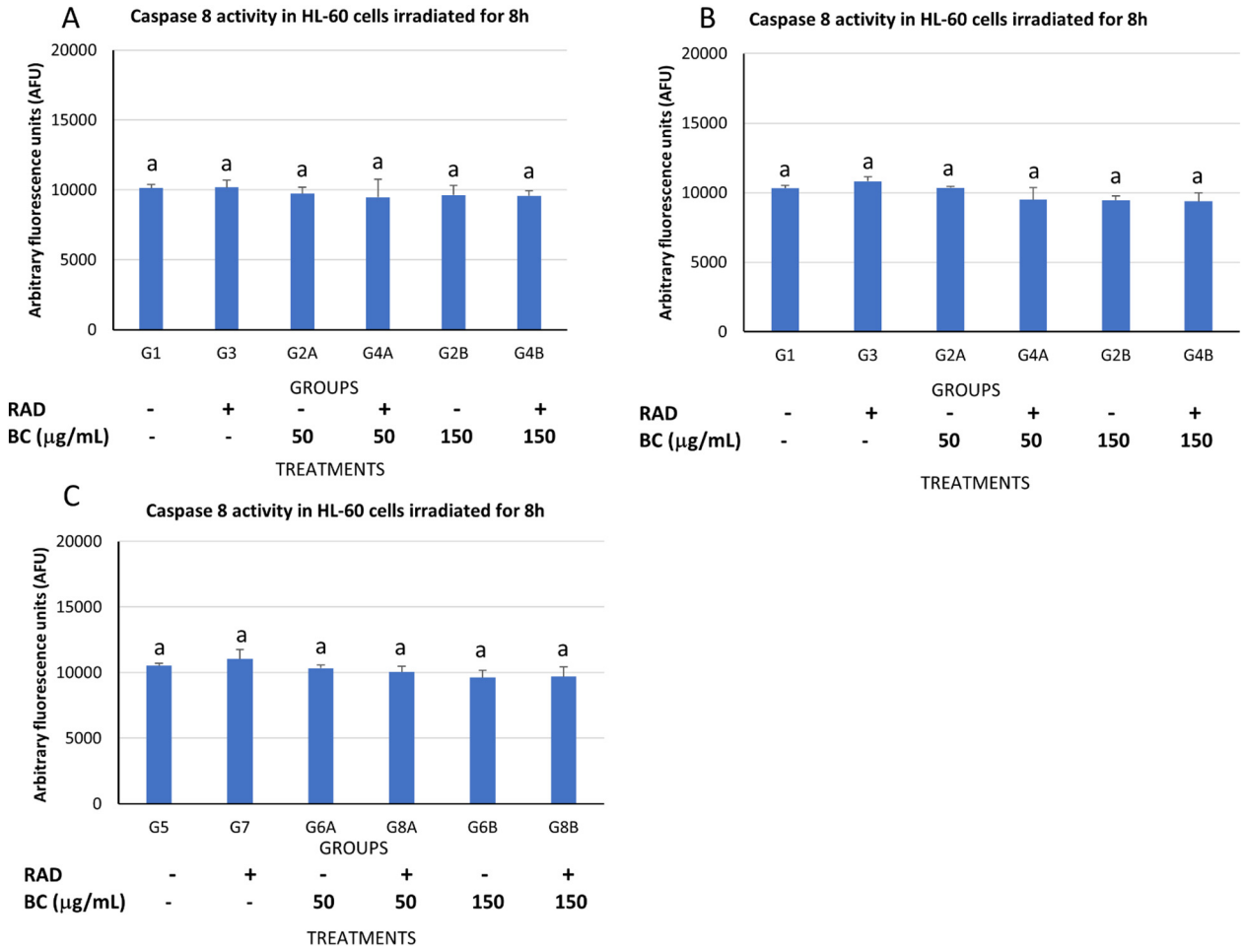

Fig. 9. Histograms showing intracellular caspase-8 activity: (A) HL-60 irradiated for 8 h. (B) HL-60 irradiated for 24 h (C) HL-60 irradiated for 48 h. The values shown are means (six samples for each group/time). Bars indicate the standard error of the mean (SEM) within each group (irradiated with/without BC, only BC or not irradiated). Different letters indicate significant differences among groups ($p < 0.05$).

significantly high levels in the promyelocytic cells in experimental groups that were irradiated for 48 h only or irradiated for 48 h and exposed to the lower dose of BC (Fig. 6B); these receptors can also trigger activation of apoptosis through the extrinsic pathway (Danial and Korsmeyer, 2004). However, the levels of caspase-8 activity did not increase significantly, indicating that effective apoptotic activation of the extrinsic pathway did not occur (Mohammadinejad et al., 2019). Caspase-8 initiates the extrinsic pathway in the execution of apoptosis, but also mediates the mechanism by which necroptosis is inhibited (Tummers and Green, 2017). Necroptosis is a form of programmed necrosis that is both morphologically and mechanistically distinct from apoptosis. The induction of necroptosis triggers various changes and will probably be suppressed by caspase 8 and thus enhanced in the absence of this protein (Wallach et al., 2014).

The pro-apoptotic caspase-3 enzyme reached significantly high levels and induced apoptosis in the HL-60 cells irradiated for 8, 24 and 48 h, as it could not be inhibited by overexpression of BCL-2a (Zhang et al., 2000). The significant levels of gene expression antioxidant at 24 h in in the groups exposed to BC, but not irradiated, (Shang et al., 2021; Sarkar et al., 2011) and in the corresponding group that was only irradiated and the significant levels of cytotoxicity in these groups at later times (Figs. A and 1B) nonetheless suggest that the BC caused caspase-dependent mitochondrial damage. The lack of caspase-8 activation, despite expression of the cell death receptor gene, indicates FAS activation but an absence of extrinsically-mediated apoptosis. This finding suggests that other cell death processes, such as necroptosis, may have taken place.

5. Conclusions

Combined exposure to 2.45 Ghz RF and to BC over a period of 48 h caused very high levels of toxicity in a HL-60 cell line and triggered an antiproliferative effect that was dependent on the BC dose and exposure time. Activation the expression of antioxidant BCL2a and initial expression of the FAS cell death receptors, with no apparent activation of caspase-8, indicated mitochondrial cell damage due to triggering of apoptosis through a caspase-dependent pathway (increased caspase-3). However, cell death did not seem to be mediated by apoptosis alone, at least not caspase-dependent apoptosis, in any of the groups. This leads us to consider that other forms of programmed cell death may be activated by one or both stressors (Barati et al., 2021). The cell damage induced in vitro by the combination of both RF and BC in promyelocytic cells indicate ineffective antimicrobial function and increased immune or autoimmune tolerance (Glencross et al., 2020).

Funding

This work was supported in part by the FEDER/Ministerio de Ciencia, Innovación Universidades-Agencia Estatal de Investigación under Project PID2020-119788RB-100.

CRediT authorship contribution statement

Rosa Ana Sueiro Benavides: Methodology, Validation, Formal analysis, Investigation, Data curation, Writing – original draft, Writing – review & editing, Supervision. **José Manuel Leiro-Vidal:** Methodology, Investigation, Resources, Supervision. **J. Antonio Rodriguez:** Software, Visualization, Supervision. **Francisco J. Ares-Pena:** Conceptualization, Resources, Supervision, Project administration, Funding acquisition. **Elena López-Martín:** Conceptualization, Methodology, Validation, Formal analysis, Investigation, Data curation, Writing – original draft, Writing – review & editing, Supervision, Project administration.

Data availability

Data will be made available on request.

Declaration of competing interest

The authors declare that they have no known competing financial interests or personal relationships that would influence the work reported in this paper.

Acknowledgements

The authors thank Rafael Fuentes for technical support for the study.

References

Adlkofer, F., 2014. Whether or not the genotoxic effects of exposure to continuous wave (CW) radio frequency electromagnetic fields (RF-EMF) in HL-60 cells are reproducible, is still an open question. Mutat. Res. Genet. Toxicol. Environ. Mutagen. 1 (771), 71–72.

Ahmad, J., Hisham, A., Alhadlaq, A., Maqsood, A., Siddiqui, Saquib, Q., Abdulaziz, A., Al-Khedhairy, Musarrat, J., Ahamed, M., 2015. Concentration-dependent induction of reactive oxygen species, cell cycle arrest and apoptosis inhuman liver cells after nickel nanoparticles exposure. Environ Toxicol. 30 (2), 137–148.

Akkaya, R., Gümüş, E., Akkaya, B., Karabulut, S., Gülmez, K., Karademir, M., Taştemur, Y., Taşkıran, A.S., 2019. Wi-fi decreases melatonin protective effect and increases hippocampal neuronal damage in pentylenetetrazole induced model seizures in rats. Pathophysiology 26, 375–379.

de Almeida Rodolpho, J.M., de Godoy, K.F., Dias de Lima Fragelli, B., Brassolatti, P., Aparecida de Castro, C., 2021. Assis,M., Speglich,C., Cancino-Bernardi, J., Longo, E., de Freitas Anibal, F.,2021. Apoptosis and oxidative stress triggered by carbon black nanoparticle in the LA-9 fibroblast. Cell Physiol Biochem. 55 (3), 364–377 26.

Arnoldussen, Y.J., Skaug, V., Aleksandersen, M., Ropstad, E., Anmarkrud, K.H., Einarsdottir, E., Chin-Lin, F., Bjørklund, C.G., Kasem, M., Eilertsen, E., Apte, R.N., Zienolddiny, S., 2018. Inflammation in the pleural cavity following injection of multi-walled carbon nanotubes is dependent on their characteristic and the presence of IL-1 genes. Nanotoxicology 12 (6), 522–538.

Asano, M., Sakaguchi, M., Tanaka, S., Kashimura, K., Mitani, T., Kawase, M., Matsumura, H., Yamaguchi, T., Fujita, Y., Tabuse, K., 2017a. Effects of normothermic conditioned microwave irradiation on cultured cells using an irradiation system with semiconductor oscillator and thermo-regulatory applicator. Sci. Rep. 7, 41244.

Asano, M., Tanaka, S., Sakaguchi, M., Matsumura, H., Yamaguchi, T., Fujita, Y., Tabuse, K., 2017b. Normothermic microwave irradiation induces death of HL-60 cells through heat-independent apoptosis. Sci. Rep. 7 (1), 11406. https://doi.org/10.1038/s41598-017-11784- 12.

Ashkenazi, A., Dixit, V.M., 1998. Death receptors: signaling and modulation. Science 281, 1305–1308.

Baisch, B.L., Corson, N.M., Wade-Mercer, P., Gelein, R., Kennell, A.J., Oberdorster, G., Elder, A., 2014. Equivalent titanium dioxide nanoparticle deposition by intratracheal instillation and whole body inhalation: the effect of dose rate on acute respiratory tract inflammation. Part Fibre Toxicol. 24 (11), 5. https://doi.org/10.1186/1743-8977-11-5.

Barati, M., Javidi, M.A., Darvishi, B., Shariatpanahi, S.P., Moosavi, Z.S.M., Ghadirian, R., Khani, T., Sanati, H., Simaee, H., Barough, M.S., Farahmand, L., Ansari, A.M., 2021. Necroptosis triggered by ROS accumulation and ca 2+ overload, partly explains the inflammatory responses and anti-cancer effects associated with 1Hz, 100 mT ELF-MF in vivo. Free Radic. Biol. Med. 169, 84–98.

Birnie, G.D., 1988. The HL60 cell line: a model system for studying human myeloid cell differentiation. Br. J. Cancer Suppl. 9, 41–45.

Bosch-Capblanch, X., Ekpereonne, E., Dongus, E., Oringanje, C.M., Eyers, J., Oftedal, J., Meremikwu, M., Röösli, M., 2022. The effects of radiofrequency electromagnetic fields exposure on human self-reported symptoms: a protocol for a systematic review of human experimental studies. Environ. Int. 158, 106953.

China, S., Mazzoleni, C., Gorkowski, K., Aike, N.A.C., Dubey, M.K., 2013. Morphology and mixing state of individual freshly emitted wildfire carbonaceous particles. Nat. Commun. 4, 2122.

Choi, H.S., Kim, J.W., Cha, Y.N., Kim, C., 2006. A quantitative nitroblue tetrazolium assay for determining intracellular superoxide anion production in phagocytic cells. J. Immunoassay Immunochem. 27, 31–44.

Chowdhury, S., Pozzer, A., Haines, A., Klingmüller, K., Münzel, T., Paasonen, P., Sharma, A., Lelieveld, J., Ch, Venkataraman, 2022. Global health burden of ambient PM 2.5 and the contribution of anthropogenic black carbon and organic aerosols. Environ Int 15 (159), 107020.

Chu, S., Li, X., Sun, N., He, F., Cui, Z., Li, Y., Liu, R., 2021. The combination of ultrafine carbon black and lead provoques cytotoxicity and apoptosis in mice lung fibroblasts through oxidative stress-activated mitochondrial pathways. Sci. Total Environ. 799 (10), 149420.

Çiğ, B., Nazıroğlu, M., 2015. Investigation of the effects of distance from sources on apoptosis, oxidative stress and cytosolic calcium accumulation vi TRPV1 channels induced by mobile phones and Wi-Fi in breast cancer cells. Biochim. Biophys. Acta 1848 (10 Pt B), 2756–2765.

Danial, N.N., 2007. BCL-2 family proteins: critical checkpoints of apoptotic cell death. Clin. Cancer Res. 13 (24), 7254–7263. https://doi.org/10.1158/1078-0432.CCR-07-1598 15.

Danial, N.N., Korsmeyer, S.J., 2004. Cell death: critical control points. Cell 116 (2), 205–219. https://doi.org/10.1016/s0092-8674(04)00046-7 PMID: 14744432.

Di, G., Gu, X., Lin, Q., Wu, S., Kim, H.B., 2018. A comparative study on effects of static electric field and power frequency electric field on hematology in mice. Ecotoxicol. Environ. Saf. 166, 109–115.

Esfandiari, N., Sharma, R.K., Saleh, R.A., Thomas Jr., A.J., Agarwal, A., 2003. Utility of the nitroblue tetrazolium reduction test for assessment of reactive oxygen species production by seminal leukocytes and spermatozoa. J. Androl. 24, 862–870.

Fabisiak, J.P., Kagan, V.E., Ritov, V.B., Johnson, D.E., Lazo, J.S., 1997. Bcl-2 inhibits selective oxidation and externalization of phosphatidylserine during paraquat-induced apoptosis. Am. J. Phys. 272, 675 follow-up of the GAZEL cohort. Environ. Int. 157,106805.

Faizan, M.I., Ahmad, T., 2021. Altered mitochondrial calcium handling and cell death by necroptosis: an emerging paradigm. Mitochondrion 57, 47–62 Review.

García-Minguillán López, O., Jiménez Valbuena, A., Maestú Unturbe, C., 2019. Significant cellular viability dependence on time exposition at ELF-EMF and RF-EMF in vitro studies. Int. J. Environ. Res. Public Health 16 (12), 208 13.

GBD, 2016. Risk Factors Collaborators. Global, regional, and national comparative risk assessment of 84 behavioural, environmental and occupational, and metabolic risks or clusters of risks, 1990–2016: a systematic analysis for the Global Burden of Disease Study 2016. Lancet 390, 10100.

Ghio, A.J., Carraway, M.S., Madden, M.C., 2012. Composition of air pollution particles and oxidative stress in cells, tissues, and living systems. J. Toxicol. Environ. Health B Crit. Rev. 15 (1), 1–21.

Glencross, D.A., Ho, T.R., Camiña, N., Hawrylowicz, C.M., Pfeffer, P.E., 2020. Air pollution and its effects on the immune system. Review. Free Radic Biol Med. 1 (151), 56–68.

Goncalves, D.M., de Liz, R., Girard, D., 2011. Activation of neutrophils by nanoparticles. Sci. World J. 11, 1877–1885. https://doi.org/10.1100/2011/768350.

González, D., Espino, J., Bejarano, I., López, J.J., Rodríguez, A.B., Pariente, J.A., 2010. Molecular and cellular biochemistry. Caspase-3 and -9 are activated inhuman myeloid HL-60 cells by calcium. Signal. 333, 151.

Guan, S., Tao, S., Huang, Y., Jin, Y., Hu, Y., Lu, J., 2020. Combined toxic effects of CBNPs and Pb on rat alveolar macrophage apoptosis and autophagy flux. Ecotoxicol. Environ. Saf. 1 (205), 111062.

Henschenmacher, B., Bitsch, A., de Las Heras, G.T., Forman, H.J., Fragoulis, A., Ghezzi, P., Kellner, R., Koch, W., Kuhne, J., Sachno, D., Schmid, G., Tsaioun, K., Verbeek, J., Wright, R., 2022. The effect of radiofrequency electromagnetic fields (RF-EMF) on biomarkers of oxidative stress in vivo and in vitro: a protocol for a systematic review. Environ. Int. 106932.

Hou, Q., Wang, M., Wu, S., Ma, X., An, G., Liu, H., Xie, F., 2015. Oxidative changes and apoptosis induced by 1800-MHz electromagnetic radiation in NIH/3T3 cells. Electromagn. Biol. Med. 34 (1), 85–92.

Hu, X., Zhou, Q., Onda, K., Toyoda, H., Hirano, T., Yuan, B., Tanaka, S., 2014. Involvement of oxidative stress associated with glutathione depletion and p3 mitogen-activated protein kinase activation in arsenic disulfide-induced differentiation in HL-60 cells. Leuk Lymphoma 55 (2), 392–404.

Jacobsen, N.R., Moller, P., Jensen, K.A., Vogel, U., Ladefoged, O., Loft, S., Wallin, 2009. Lung inflammation and genotoxicity following pulmonary exposure to nanoparticles in ApoE-/- mice. Part Fibre Toxicol. 12 (6), 2.

Johnston, H., Brown, D.M., Kanase, K., Euston, M., Gaiser, B.K., Robb, C.T., Dyrynda, E., Rossi, A.G., Brown, E.R., Stone, V., 2015. Mechanism of neutrophil activation and toxicity elicited by engineered nanomaterials. Toxicol. in Vitro 29 (5), 1172–1184.

Kagan, V.E., Fabisiak, J.P., Shvedova, A.A., Tyurina, Y.Y., Tyurin, V.A., Schor, N.F., Kawai, K., 2000. Oxidative signaling pathway for externalization of plasma membrane phosphatidylserine. FEBS Lett. 477 (1-2), 1–7 14.

Kamali, K., Taravati, A., Sayyadi, S., Gharib, F.Z., Maftoon, H., 2018. Evidence of oxidative stress after continuous exposure to Wi-Fi radiation in rat model. Environ. Sci. Pollut. Res. Int. 25 (35), 35396–35403.

Keeble, J.A., Gilmore, A.P., 2007. Apoptosis commitment – translating survival signals into decisions on mitochondria. Cell Res. 17, 976–984.

Kim, J.H., Kang, D.J., Bae, J.S., Lee, J.H., Jeon, S., Choi, H.D., Kim, N., Kim, H.G., Kim, H.R., 2021. Activation of matrix metalloproteinases and FoxO3a in HaCaT keratinocytes by radiofrequency electromagnetic field exposure. Sci. Rep. 11 (1), 7680.

Kobayashi, S.D., Malachowa, N., DeLeo, F.R., 2017. Influence of microbes on neutrophil life and death. Review Front. Cell Infect Microbiol. 7, 159.

Kostoff, R.N., Lau, C.G.Y., 2017. Modified health effects of non-ionizing electromagnetic radiation combined with other agents reported in the biomedical literature. In: Geddes, C. (Ed.), Microwave Effects on DNA and Proteins. Springer, Cham, pp. 97–157.

Kovacic, P., Somanathan, R., 2008. Integrated approach to immunotoxicity: electron transfer, reactive oxygen species, antioxidants, cellsignaling, and receptors. Recept Signal Transduct. Res. 28 (4), 323–346.

Kovacic, P., Somanathan, R., 2010. Electromagnetic fields: mechanism, cell signaling, other bioprocesses, toxicity, radicals, antioxidants and beneficial effects. Rev.J. Recept Signal Transduct. Res. 30 (4), 214–226.

Koyama, S., Narita, E., Suzuki, Y., Taki, M., Shinohara, N., Miyakoshi, J., 2015. Effect of a 2.45-GHz radiofrequency electromagnetic field on neutrophil chemotaxis and phagocytosis in differentiated human HL-60 cells. J. Radiat. Res. 56 (1), 30–36.

Lee, S., Johnson, D., Dunbar, K., Dong, H., Ge, X., Kim, Y.C., Wing, C., Jayathilaka, N., Emmanuel, N., Zhou, C.Q., Gerber, H.L., Tseng, C.C., Wang, S.M., 2005. 2.45 GHz radiofrequency fields alter gene expressionin cultured human cells. FEBS Lett. 579 (21), 4829–4836 29.

Lippi, G., Danese, E., Brocco, G., Benati, M., Salvagno, G.L., Montagnana, M., Franchini, M., 2016. Thirty-minutes' exposure to smartphone call triggers neutrophil activation in vitro. Clin. Chem. Lab. Med. 54 (9), 1497–1501.

Long, C.M., Nascarella, M.A., Valberg, P.A., 2013. Carbon black vs. Black carbon and other airborne materials containing elemental carbon: physical and chemical distinctions. Environ. Pollut. 181, 271–286.

López-Martín, E., Jorge-Barreiro, F.J., Relova-Quintero, J.L., Salas-Sánchez, A.A., Ares-Pena, F.J., 2021. Exposure to 2.45GHz radiofrequency modulates calcitonin-dependent activity and HSP-90 protein in parafollicular cells of rat thyroid gland. Tissue Cell. F;68. https://doi.org/10.1016/j.tice.2020.101478.

Magalhaes, S., Baumgartner, J., Weichenthal, S., 2018. Impacts of exposure to black carbon, elemental carbon, and ultrafine particles from indoor and outdoor sources on blood pressure in adults: a review of epidemiological evidence. Review Environ. Res. 161, 345–353.

Magnusson, C., Vaux, D., 2000. Signalling by CD95 and TNF receptors: not only life and death. Immunol Cell Biol Cell Res. 10 (3), 213–220.

Mohammadinejad, R., Moosavi, M.A., Tavakol, S., Vardar, D.Ö., Hosseini, A., Rahmati, M., Dini, L., Hussain, S., Mandegary, A., Klionsky, D.J., 2019. Necrotic, apoptotic and autophagic cell fates triggered by nanoparticles. Autophagy 15 (1), 4–33. https://doi.org/10.1080/15548627.2018.1509171.

Murphy, F.A., Poland, C.A., Duffin, R., Donaldson, K., 2013. Length-dependent pleural inflammation and parietal pleural responses after deposition of carbon nanotubes in the pulmonary airspaces of mice. Nanotoxicology (6), 1157–1167.

Nazıroğlu, M.B., Ciğ, S., Doğan, A.C., Uğuz, S., Dilek, D., Faouzi, S., 2012. 2.45-GHz wireless devices induce oxidative stress and proliferation through cytosolic Ca2 + influx in human leukemia cancer cells. Int. J. Radiat. Biol. 88, 449–456.

Noorimotlagh, Z., Azizi, M., Pan, H., Mami, S., Mirzaee, S.A., 2021. Association between air pollution and multiple sclerosis: a systematic review.Review. Environ. Res. 196, 110386.

Offer, S., Hartner, E., DiBucchianico, S., Bisig, C., Bauer, S., Pantzke, J., Zimmermann, E.J., Cao, X., Binder, B.S., Kuhn, E., Huber, A., Jeong, S., Käfer, U., Martens, P., Mesceriakovas, A., Bendl, Buchholz, B.D.A., Gat, D., Hohaus, T., Rastak, N., Jakobi, G., Kalberer, M., Kanashova, T., Hu, Y., Ogris, C., Marsico, A., Theis, F., Pardo, M., Gröger, T., Oeder, S., Orasche, J., Paul, A., Zhang, T.Z., Adam, T., Sippula, O., Jürge, M., Krei, Schnelle, Czech, H., KiendlerScharr, A., Rudich, Y., Zimmermann, R., 2022. Effect of atmospheric aging on soot particle toxicity in lung cell models at the air-liquid interface: differential toxicological impacts of biogenic and anthropogenic secondary organic aerosols (SOAs). Environ Health Perspect. 130 (2), 27003.

Özsobacı, N.P., Ergün, D.D., Durmuş, S., Tunçdemir, M., Uzun, H., Gelişgen, R., Özçelik, D., 2018. Selenium supplementation ameliorates electromagnetic field-induced oxidative stress in the HEK293 cells. J. Trace Elem. Med. Biol. 50, 572–579.

Pall, M.J., 2018. Wi-fi is an important threat to human health. Environ. Res. 164, 405–416.

Palumbo, R., Capasso, D., Brescia, F., Mita, P., Sarti, M., Bersani, F., Scarfi, M.R., 2006. Effects on apoptosis and reactive oxygen species formation by jurkat cells exposed to 50 hz electromagnetic fields. Bioelectromagnetics 27 (2), 159–162.

Panagopoulos, D.J., Karabarbounis, A., Yakymenko, I., Chrousos, G.P., 2021. Human-made electromagnetic fields: ion forced-oscillation and voltage-gated ion channel dysfunction, oxidative stress and DNA damage (Review). J. Oncol. 59 (5), 92.

Pilla, A., Fitzsimmons, R., Muehsam, D., Wu, J., Rohde, C., Casper, D., 2011. Electromagnetic fields as first messenger in biological signaling: application to calmodulin-dependent signaling in tissue repair. Biochim. Biophys. Acta 1810 (12), 1236–1245.

Poland et al., n.d.C.A. Poland R. Duffin I. Kinloch A. Maynard W.A. Wallace A. Seaton V. Stone S. Brown Pulmonary airspaces of mice. n.d. Nanotoxicology. 7(6), 1157-67.

Rao, X., Jixin, Z., Brook, R.D., Rajagopalan, S., 2018. Effect of particulate matter air Pollution on cardiovascular oxidative stress pathways. Antioxid. Redox Signal. 28 (9), 797–818.

Rebuli, M.E., Brocke, S.A., Jaspers, I., 2021. Impact of inhaled pollutants on response to viral infection in controlled exposures. Rev.J. Allergy Clin. Immunol. 148 (6), 1420–1429.

Reed, J.C., 2000. Mechanisms of apoptosis. Am J Pathol 157, 1415–1430 Eeview of epidemiological evidence. Env. Res. 161, 345–353.

Rituraj, N., Thakur, K.A., 2017. The toxicological mechanisms of environmental soot (Black Carbon) and carbon black: focus on oxidative stress and inflammatory pathways. Rev. Front. Immunol. 30 (8), 763.

Röösli, M., Frei, P., Mohler, E., Hug, K., 2010. Systematic review on the health effects of exposure to radiofrequency electromagnetic fields from mobile phone base stations. Bull. World Health Organ. 88 (12), 887–896F 1.

Russell, W.M.S., Burch, R.L., 2005. The principles of humane experimental technique. Baltimore, S.2018. Nanotoxicology 12 (6), 522–538.

Salas-Sánchez, A.A., López-Furelos, A., Rodríguez-González, J.A., Ares-Pena, F.J., López-Martín, M.E., 2019. Validation of potential effects on human health of in vivo experimental models studied in rats exposed to sub-thermal radiofrequency. Possible health risks due to the interaction of electromagnetic pollution and environmental particles. IEEE Access 7, 79186–79198.

Salas-Sánchez, A.A., Rauch, J., López-Martín, M.E., Rodríguez-González, J.A., Franceschetti, G., Ares-Pena, F.J., 2020. Feasibility study on measuring the particulate matter level in the atmosphere by means of yagi-Uda-like antennas. Sensors (Basel 20 (11), 3225 5.

Santini, S.J., Cordone, V., Falone, S., Mijit, M., Tatone, C., Amicarelli, F., Di Emidio, G., 2018. Role of mitochondria in the oxidative stress induced electromagnetic fields: focus on reproductive systems. Oxidative Med. Cell. Longev. 8 (2018), 5076271.

Sarkar, A., Das, J., Manna, P., Sil, P.C., 2011. Nano-copper induces oxidative stress and apoptosis in kidney via both extrinsic and intrinsic pathways. Toxicology 290 (2–3), 208–217 18.

Schuermann, D., Mevissen, M., 2021. Manmade electromagnetic fields and oxidative stress biological effects and consequences for health. Int. J. Mol. Sci. 22 (7), 3772.

Shang, Y., Xue, W., Kong, J., Chen, Y., Qiu, X., An, X., Li, Y., Wang, H., An, J., 2021. Ultrafine black carbon caused mitochondrial oxidative stress, mitochondrial. Ultrafine black carbon caused mitochondrial oxidative stress, mitochondrial dysfunction and mitophagy in SH-SY5Y cells. Sci. Total Environ. 20 (813), 151899.

Speit, G., Gminski, R., Tauber, R., 2013. Genotoxic effects of exposure to radiofrequency electromagnetic fields (RF-EMF) in HL-60 cells are not reproducible. Mutat Res. 755 (2), 163–166. https://doi.org/10.1016/j.mrgentox.2013.06.014 201,15.

Su, L.J., Zhang, J.H., Gomez, H., Murugan, R., Hong, X., Xu, D., Jiang, F., Peng, Z.Y., 2019. Reactive oxygen species-induced lipid peroxidation in apoptosis autophagy, and ferroptosis. Oxidative Med. Cell. Longev. 13, 5080843.

Sueiro-Benavides, R.A., Leiro-Vidal, J.M., Salas-Sánchez, A.Á., Rodríguez-González, J.A., Ares-Pena, F.J., López-Martín, M.E., 2021. Radiofrequency at 2.45 GHz increases toxicity, proinflammatory and pre apoptotic activity caused by black cabon in the RAW 264.7 macrophage cell line. Science of The Total Environment 765, 15142681.

Sun, Y., Zong, L., Gao, Z., Zhu, S., Tong, J., Cao, Y., 2017. Mitochondrial DNA damage and oxidative damage in HL-60 cells exposed to 900MHz radiofrequency fields. Mutat. Res. 797–799, 7–14.

Tök, L., Nazıroğlu, M., Doğan, S., Kahya, M.C., Tök, O., 2014. Effects of melatonin on wi-fi-induced oxidative stress in lens of rats. Indian J. Ophthalmol. 62 (1), 12–15. https://doi.org/10.4103/0301-4738.126166.

Tummers, B., Green, D.R., 2017. Caspase-8: regulating life and death. Immunol. Rev. 277 (1), 76–89.

Vagdatli, E., Konstandinidou, V., Adrianakis, N., Tsikopoulos, I., Tsikopoulos, A., Mitsopoulou, K., 2014. Effects of electromagnetic fields on automated blood cell measurements. J Lab Autom. 19 (4), 362–365 Aug.

Verbeek, J., Oftedal, G., Feychting, M., Rongen, E., Scarfi, M.R., Wong, S.M.R., Deventer, E., 2021. Prioritizing health outcomes when assessing the effects of exposure to radiofrequency electromagnetic fields: a survey among experts. Environ. Int. 146, 106300.

Verdon, R., Gillies, S.L., Brown, D.M., Henry, T., Tran, L., Tyler, C.R., Rossi, A.G., Stone, V., Johnston, H.J., 2021. Neutrophil activation by nanomaterials in vitro: comparing strengths and limitations of primary human cells with those of an immortalized (HL-60) cell line. Nanotoxicology 15 (1), 1–20.

Wallach, D., Kang, T.B., Yang, S.H., Kovalenko, A., 2014. The in vivo significance of necroptosis: lessons from exploration of caspase-8 function. Cytokine Growth Factor Rev. 25 (2), 157–165.

Wang, D., Sennari, Y., Shen, M., Morita, K., Kanazawa, T., Yoshida, Y., 2020. ERK is involved in the differentiation and function of dimethyl sulfoxide-induced HL-60 neutrophil-like cells, which mimic inflammatory neutrophils. Int. Immunopharmacol. 84, 106510.

Wang, Q., Schwarz, J.P., Cao, J., Gao, R., Fahey, D.W., Hu, T., et al., 2014. Black carbon aerosol characterization in a remote area of Qinghai-tibetan plateauWestern China. Sci Total Environ 247 (9–480), 151–158.

Watson, A.Y., Valberg, P.A., 2001. Carbon black and soot: two different substances. AIHAJ. 62 (2), 218–228.

Westphal, G.A., Schremmer, I., Rostek, A., Loza, K., Rosenkranza, N., Brüning, T., Epple, M., Bünger, J., 2015. Particle-induced cell migration assay (PICMA): a new in vitro assay for inflammatory particle effects based on permanent cell lines. Toxicol. In Vitro 29 (015), 997–1005.

Wócik-Piotrowicz, K., Kaszuba-Zwoińska, J., Rokita, E., Thor, P., Chrobik, P., Nieckarz, Z., Michalski, J., 2014. Influence of static and alternating magnetic fields on U937 cell viability. Folia Med.Cracov. 54 (4), 21–33.

Wójcik-Piotrowicz, K., Kaszuba-Zwoińska, J., Rokita, E., Thor, P., 2016. Cell viability modulation through changes of Ca (2+)-dependent signalling pathways review. Prog. Biophys. Mol. Biol. 121 (1), 45–53.

Wojcik-Piotrowicz, K., Kaszuba-Zwoinska, J., Rokita, E., Nowak, B., Thor, P., 2017. Changes in U937 cell viability induced by stress factors - possible role of calmodulin. J. Physiol. Pharmacol. 68 (4), 629–636.

Yang, J., Sakhvidi, M.J.Z., de Hoogh, K., Vienneau, D., Siemiatyck, J., Zins, M., Goldberg, M., Chen, J., Lequy, E., Jacquemin, B., 2021. Long-term exposure to black carbon and mortality: a 28-year follow-up of the GAZEL cohort. Environ. Int. 157, 106805.

Youle, R.J., Strasser, A., 2008. The BCL-2 protein family: opposing activities that mediate cell death. Nat.Rev. Mol. Cell Biol. 9 (1), 47–59.

Zhang, M., Zhang, H.Q., Xue, S.B., 2000. Effect of Bcl-2 and caspase-3 on calcium distribution in apoptosis of HL-60 cells. Cell Res. 10 (3), 213–220.

Zielinski, J., Ducray, A.D., Moeller, A.M., Murbach, M., Kuster, N., Mevissen, M., 2020. Effects of pulse-modulated radiofrequency magnetic field (RF-EMF) exposure on apoptosis, autophagy, oxidative stress and electron chain transport function inhuman neuroblastoma and murine microglial cells. Toxicol. in Vitro 68, 104963.